

Asset Management in Smart Grids Using Improved Dissolved Gas Analysis

V. Srinivasan

Research Scholar
Department of Electrical and
Electronics Engineering
Kalasalingam University
Krishnankoil, Srivilliputtur (via),
Virudhunagar District
Tamilnadu, India

B. Subathra, Seshadhri Srinivasan

Sr.Associate Professor, Professor
Kalasalingam University
Krishnankoil, Srivilliputtur (via),
Virudhunagar District
Tamilnadu, India

S.Kannan

Professor and Head,
Department of Electrical and
Electronics Engineering
Ramco Institute of Technology
Virudhunagar District
Tamil Nadu, India

Abstract— Asset Management Systems (AMS) are pivotal to build reliable and safe smart grids. An important function of AMS is the monitoring and diagnosis of the power transformers. Various tests are performed on power transformers to detect incipient faults. Among the available methods, Dissolved Gas Analysis (DGA) has been widely used and shown promise. However, interpreting the results of the DGA is challenging due to the availability of wide variety of methods such as Rogers ratio, Doernenburg ratio, key gas procedure of IEEE, Basic gas ratio and Duval triangle methods of IEC. The accuracy of the interpretation methods influences AMS performance leading to reliability issues in the grid. This investigation compares the accuracy of Duval method and basic gas ratio method to detect transformer faults from real-time fault data obtained from power transformers. Our results on data obtained from Electrical Research and Development Association for seven transformer incipient faults shows that the Duval method is accurate than the basic gas ratio method for identifying incipient transformer fault based on DGA results. Further, the basic gas ratio was not able to detect two of the seven faults. These results illustrate the need to integrate Duval method to detect power transformer faults within AMS.

Keywords—Transformer Condition Monitoring, Asset Management Systems, Dissolved Gas Analysis (DGA), Duval, basic gas ratio method.

I. INTRODUCTION

Power Transformers are vital equipment in the electric grid and their outage leads to significant economic loss. Further, replacement time of power transformer is quite high due to cost and logistics difficulties. Consequently, condition monitoring and fault-diagnosis of power transformers have received significant attention. The importance of power transformer condition monitoring can be understood from the various tests such as the insulation resistance, tan-delta, oil quality inspection, winding resistance test, dissolved gas analysis (DGA), and so on, that are conducted at regular intervals by utilities to avoid outages. Although, many tests are conducted on transformers, DGA has emerged as a promising solution, due to their ability to detect incipient faults and possible failures. However, interpreting DGA results is still challenging due to the availability of various methods such as Duval, basic gas ratio, Rogers ratio, Doernenburg ratio, and key gas procedure (see, [1]-[3] and references therein). Further, the accuracy of these methods

differ for a given fault. For instance, the accuracy of the methods for the seven faults described in Table 1 has not been studied extensively in literature. However, such a comparison is required for building future Asset Management Systems (AMS). Therefore, the accuracy of these interpretation methods in detecting incipient faults and predicting failures for enhancing the capabilities of AMS needs to be studied.

TABLE 1
OCCURRED FAULTS

Tr. Case	Actual fault occurred
1	hot-spot on connecting lead due to bolted joint loose connection
2	melting of core-stamping bolt
3	arcing between high voltage leads
4	arcing between LT bus bars
5	inter-turn fault
6	arcing at OLTC (on-load tap changer) contact
7	arcing in diverter switch

The accuracy of DGA interpretation methods for diagnosing faults has been studied by researchers and some useful comparisons have been reported in literature. As reviewing the complete literature is not within the scope of this paper; here a brief idea on significant results is presented. The authors in [2], used key gas ratio and basic gas ratio methods for diagnosing power transformer faults using DGA results. Further, the investigation developed a fuzzy inference system for improving the fault-diagnosis and detection of thermal faults using fuzzy has been studied. Although, this method is an improvement in detecting multiple faults, the approach suffers from the efficacy of the DGA interpretation methods in detecting faults. The investigation in [4] studied the use of Rogers and IEC -ratio methods for power transformer fault detection using artificial neural network using data from 30 faulted transformers. The investigation concluded that both the ratio methods are effective and simple, as the volume of the oil involved in the dissolution of the gas is not required. Though, the method is a progress towards developing expert systems for transformer condition monitoring, accuracy of inference method has not been studied. Importance of inference method accuracy can be understood in the light of results of investigation [5], that used Roger's ratio to interpret

DGA results, and concluded that the efficiency of the method in detecting incipient faults to be 45-52%. Reading the results of the investigation [4] and [5] in unison reveals that, while it is essential to harness the features of computational intelligence in building expert systems for transformer condition monitoring, their performance is however dictated by the accuracy of the DGA inference method. This necessitates studying the accuracy of the inference methods for various faults envisaged in a power transformer. Seeing, the potential of accuracy of inference methods in designing expert systems that can be used in building dependable AMS, the authors in [3], studied the accuracy for 92 common faults in power transformers. Further, the investigation concluded that Duval method showed good accuracy in detecting incipient faults. However, comparison of Duval and gas ratio method that have competing accuracies for detecting faults listed in Table 1, has not been studied in literature extensively. In particular, accuracy of these methods studying incipient and operating faults has not been studied. Motivated by this research gap, this investigation aims to determine the accuracy of two methods: Duval and basic gas ratio in detecting incipient and operating faults. The two methods have been selected due to their competing accuracies and absence of results comparing both these approaches.

To reach the objectives of this investigation, first DGA data from seven faulted transformer is collected. Then computations that perform Duval and gas ratio method are applied to the results to detect the faults. The obtained results are compared with the actual faults to draw conclusions on the accuracy of the interpretation approaches. Our results show that the accuracy of Duval method in detection of power transformer faults is quite high compared to gas ratio method.

The investigation is organized into five sections. Section II reviews the gas ratio and Duval method. The condition monitoring of transformer and the DGA data from faulted transformers is presented in section III. The fault-case studies and results are presented in section IV. Conclusions are drawn from the obtained results in Section V.

II. REVIEW OF DISSOLVED GAS BY BASIC GAS RATIO AND DUVAL TRIANGLE

The DGA results of the failed transformers obtained from the laboratory can be analyzed by both the IEC basic gas ratio method and Duval triangle method

A. IEC basic gas ratio method

In IEC basic gas ratio method, DGA results are used to determine the C_2H_2/C_2H_4 , CH_4/H_2 , C_2H_4/C_2H_6 gas ratios. DGA interpretation in Table 2 can be used to detect faults based on the gas ratio from the failed transformers.

TABLE 2
DGA INTERPRETATION

Case	Characteristic fault	C_2H_2/C_2H_4 in ppm	CH_4/H_2 in ppm	C_2H_4/C_2H_6 in ppm
PD	Partial discharges	NS	<0.1	<0.2
D1	Discharges of low energy	>1	0.1-0.5	>1
D2	Discharges of high energy	0.6-2.5	0.1-1	>2
T1	Thermal fault $t < 300^\circ C$	NS	1 but NS	<1
T2	Thermal fault $300^\circ C < t < 700^\circ C$	<0.1	>1	1-4
T3	Thermal fault $t > 700^\circ C$	<0.2	>1	>4

NS = Non-significant whatever the value

B. IEC Duval triangle method:

In Duval method, the gas concentration values are used to construct the coordinates of the triangle shown in Figure 1. The Duval coordinates are computed by using (1-3).

$$\%C_2H_2 = (100x)/(x+y+z) \text{ for } x = [C_2H_2] \text{ in ppm.} \quad (1)$$

$$\%C_2H_4 = (100y)/(x+y+z) \text{ for } y = [C_2H_4] \text{ in ppm.} \quad (2)$$

$$\%CH_4 = (100z)/(x+y+z) \text{ for } z = [CH_4] \text{ in ppm.} \quad (3)$$

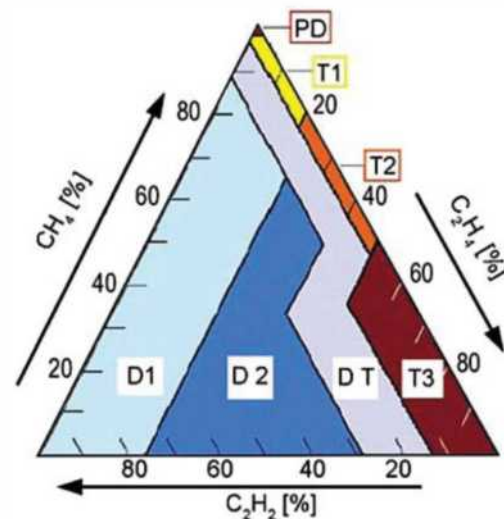


Figure 1: Duval triangle

After constructing the Duval triangle the faults are identified from the intersections of the coordinates computed from (1-3). This triangle forms the basis of analysis for the faults. The various faults that can be studied using Duval coordinates/gas ratio are defined in the standard IEC 60599 and are illustrated in Table 3, and Table 4, respectively.

TABLE 3
TYPICAL FAULTS IN POWER TRANSFORMERS

Type	Fault	Examples
PD	Partial discharges	Discharges in gas-filled cavities resulting from incomplete impregnation, high-humidity in paper, oil super saturation or cavitation, and leading to X-wax formation
D1	Discharges of low energy	Sparkling or arcing between bad connections of different or floating energy potential, from shielding rings, toroids, adjacent disks or conductors of winding, broken brazing or closed loops in the corona Discharges between clamping parts, bushing and tank, high voltage and ground within windings, on tank walls Tracking in wooden blocks, glue of insulating beam, winding spacers, Breakdown of oil, selector breaking current
D2	Discharges of high energy	Flashover, tracking, or arcing of high local energy or with power follow-through Short circuits between low voltage and ground, connectors, windings, bushings and tank, copper bus and tank, windings and core, in oil duct, turret. Closed loops between two adjacent conductors around the main magnetic flux, insulated bolts of core, metal rings holding core legs
DT	Thermal and electrical faults	Mixture of thermal and electrical faults
T1	Thermal fault $t < 300^{\circ}\text{C}$	Overloading of the transformer in emergency situations Blocked item restricting oil flow in windings Stray flux in damping beams of yokes
T2	Thermal fault $300^{\circ}\text{C} < t < 700^{\circ}\text{C}$	Defective contacts between bolted connections (particularly between aluminium busbar), gliding contacts, contacts within selector switch (pyrolitic carbon formation), connections from cable and draw-rod of bushing Circulating currents between yoke clamps and bolts, clamps and

		laminations, in ground wiring, defective welds or clamps in magnetic shields Abraded insulation between adjacent parallel conductors in windings
T3	Thermal fault $t > 700^{\circ}\text{C}$	Large circulating currents in tank and core. Minor currents in tank walls created by a high uncompensated magnetic field Shorting links in core steel laminations

In addition to diagnosing transformer faults, DGA can be used to diagnose faults in switching equipment and accessories. The type of faults that are defined within the standard IEC 60599 is shown in Table 4.

TABLE 4
TYPICAL FAULTS IN SWITCHING DEVICES

Type	Fault	Examples
D1	Discharges of low energy	Normal operation of OLTC, selectors Arcing on off-load selector switch ring, OLTC connections
D2	Discharges of high energy	Switch contacts do not reach their final position but stop halfway, due to a failure of the rotating mechanism, inducing a spark over discharge Arcing on off-load selector switch ring, OLTC connections, of high energy or with power follow-through, with failure often transmitted to transformer windings
T3	Thermal fault	Increased resistance between contacts of OLTC or change-over selector, as a result of pyrolitic carbon growth, selector deficiency or a very large number of operations

III. CONDITION MONITORING AND DGA DATA

The transformer condition monitoring method using DGA test results is shown in Figure 2. The transformer oil collected from the transformer is the input to the DGA test, while the composition of dissolved gases in the transformer oil is the output. An analysis of the gas compositions gives information on possible transformer faults and gas ratio/Duval coordinates are used to this extent. This information is used by the diagnostic methods to detect the faults. As stated earlier, numerous methods are available in diagnosing the DGA results and their accuracy differs for a given fault. The DGA results and the gas ratios obtained from the laboratory for the

seven cases of faults studied in the investigation are given in Table 5 and Table 6, respectively. The gas ratios are analyzed with the DGA interpretation (Table 2) and the corresponding type of fault is determined as shown in Table 8.

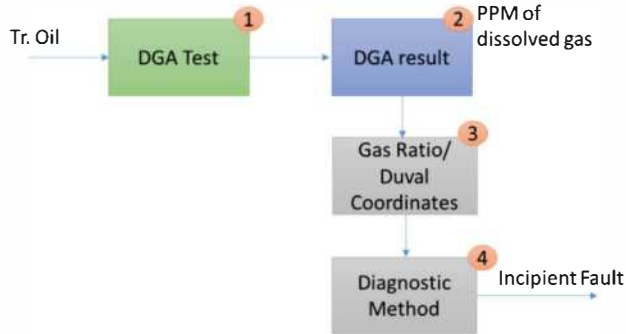


Figure 2: DGA based transformer condition monitoring system

TABLE 5
DGA RESULTS FROM THE FAULTED POWER TRANSFORMERS

Tr. Case	DGA results in ppm						
	H ₂	CH ₄	C ₂ H ₂	C ₂ H ₄	C ₂ H ₆	CO	CO ₂
1	1049	6986	1476	39998	6462	40773	949998
2	45	296	4	2228	1292	68	1458
3	2113	319	408	469	82	1632	4190
4	161	34	90	55	3	118	1151
5	821	1030	2	48	25	213	522
6	1064	1409	133	2046	1436	4779	1152
7	72	273	0	326	35	67	1383

TABLE 6
GAS RATIOS

Tr. Case	Gas ratios				
	C ₂ H ₂ / C ₂ H ₄	CH ₄ / H ₂	C ₂ H ₄ /C ₂ H ₆	CO ₂ /CO	C ₂ H ₂ / H ₂
1	0.04	6.6	6.19	2.3	1.407
2	0.002	6.58	1.72	21.44	0.088
3	0.87	0.151	5.72	2.57	0.193
4	1.63	0.211	18.33	9.75	0.56
5	0.042	1.25	1.92	2.45	0.003
6	0.065	1.32	1.42	0.24	0.125
7	0.0	3.79	9.3	20	0

The Duval coordinates constructed from the DGA test is shown in Table 7 and used as the basis to study transformer faults. These Gas ratios and Duval co-ordinates are analysed in the Duval triangle (Figure 1) and the corresponding type of fault is determined as shown in Table 8.

TABLE 7
DUVAL CO-ORDINATES

Tr. Case	Duval co-ordinates		
	% C ₂ H ₂	% C ₂ H ₄	%CH ₄
1	3.05	82.54	14.4
2	0.16	88.14	11.7
3	34.11	39.21	26.67
4	50.27	30.72	18.99
5	0.185	4.44	95.37
6	4.12	63.38	32.5
7	0.16	54.33	45.5

TABLE 8
FAULTS

Tr. Case	Actual fault occurred	Fault found by gas ratio	Fault found by Duval triangle
1	Hot spot on one connecting leads due to joint loose connection	T3	T3
2	Bolt on stamping got melted	T2	T3
3	Sparking on HT leads	D2	D2
4	Arcing between LT busbars	D1	D2
5	Damaged winding	T2	T1
6	Arcing at contacts (OLTC)	T2	T3
7	Arcing in diverter switch (OLTC)	T1	T3

IV. FAULT ANALYSIS

This section computes the faults using the Duval and basic gas ratio method using the DGA results of seven faulted transformers from Electrical Research and Development Association (ERDA). Computations based on Duval and basic gas ratio methods were used to analyse the faults and the finding are reported in this section.

A. Case 1: Hot-spot in connecting lead due to bolted joint loose connection

The hot spot in one of the connecting lead due to joint loose connection causes power transformer failure. Further, it results in pitting and melting of the mild steel bolt. As the melting point of mild steel is greater than 700°C, the fault is in the T3 zone of the transformer. One can find from our analysis that both Duval and basic gas ratio methods were able to detect the faults as illustrated in Table 8.

B. Case 2: Melting of core stamping bolt

The second case of fault considered is the melting of core stamping bolt as shown in Figure 3. Since, the transformer grade stainless steel bolt melting point is above 1500°C; the fault region T3 identified by Duval suggests that the fault has been identified accurately. But, our computation with basic gas ratio reveals that the method cannot capture this type of fault accurately.

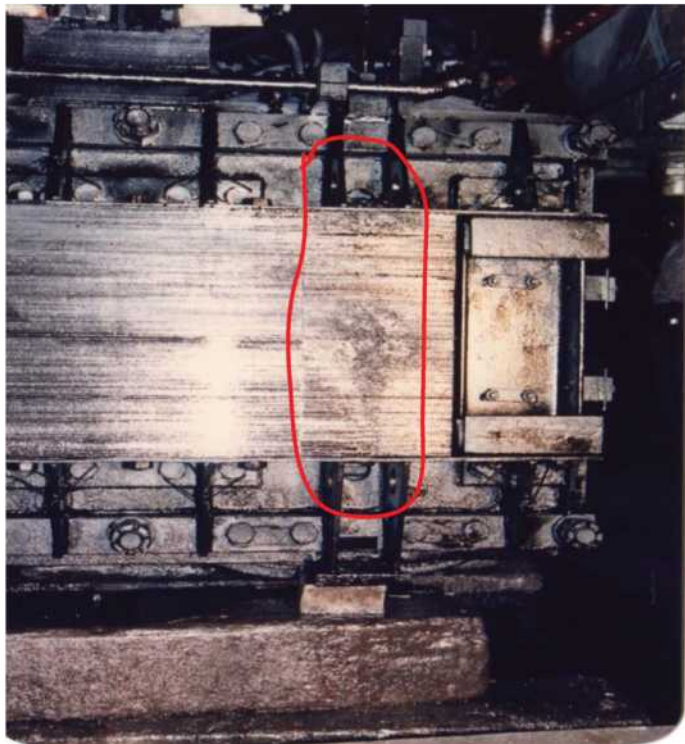


Figure 3: Melting of core stamping bolt

C. Case 3: Arcing between high voltage leads

The third case considered is the arcing between high voltage leads due to insulation failure resulting in a short circuit between two phases that is caused by heavy current flow which corresponds to high energy discharge D2 of Table 3. Our calculations with Duval and basic gas ratio illustrates that both these methods were able to detect the fault accurately as illustrated from Table 8.

D. Case 4: Arcing between LT bus bars

The fourth case of failure considered in our analysis is the arcing between the LT bus bars due to insulation failure. This results in increased current flow due to short circuiting of two phases with a high energy discharge. This fault corresponds to D2 of Table 3. Our computations with DGA results reveal

that only Duval method is able to capture this fault, while basic gas ratio method fails to diagnose it.

E. Case 5: Inter-turn fault

The inter turn fault is most common in power transformers that leads to insulation of the winding to be overheated and decolorized. The fault results due to thermal breakdown in the insulation resistance of the oil immersed transformer windings (class-B insulation) which will withstand a temperature of up to 130°C. From our computations, one can find that the Duval method computed the fault to be in zone T1 is more appropriate than the T2 detected by gas ratio method. This illustrates that the Duval method is able to diagnose inter-turn fault more accurately than the basic gas ratio method.

F. Case 6: Arcing at OLTC contacts

The sixth fault analyzed is the improper contact at OLTC slider that happens due to switching of transformer taps (Figure 4). The faulted transformer is subjected to arcing and melting of copper contact surfaces. This leads to a thermal fault. The Duval method predicted the fault to be in T3 that corresponds to thermal fault. On the other hand, the basic gas ratio method predicted the failure to be in zone T2, which is not included in the switching and equipment accessories fault (Table 4). Therefore, our computations establish that Duval is more accurate and efficient in detecting arcing at OLTC contacts.



Figure 4: Arcing at OLTC contacts

G. Case 7: Arcing in diverter switch

Arcing in the diverter switch is an external fault that leads to thermal fault. This is an operation fault that can lead to failures. Our computations on power transformer indicated that, while Duval method was able to diagnose the fault, the basic gas ratio method failed to detect this fault. One can

conclude that the Duval method is more suitable for detecting such external faults from the DGA results.

Our analysis on the DGA data obtained from the transformer and computations performed using Duval and basic gas ratio method illustrated the accuracy of the methods. While, Duval was able to capture all seven faults successfully; the basic gas ratio was not able to capture five out of seven faults. It is to be noted here that, the case 6 of the fault is not even listed in the possible faults that can be detected by basic gas ratio. However, Duval computed the fault accurately. This naturally suggests us to conclude that Duval is a more accurate method in detecting faults from DGA results and affirms the finding of the investigation [1]. Therefore, Duval method could well turn out to be the method required for building dependable AMS in future.

V. CONCLUSION

The paper compared the accuracy of two DGA interpretation methods in practice: Duval and basic gas ratio method. The study was based on seven faults (incipient, operational, and external) on the power transformers. The DGA results of the faulted transformers were obtained from Electrical Research and Development Association (ERDA) and studied in our investigation. Computations were performed on the DGA results using both Duval and basic gas ratio method. Our computations illustrated that Duval was successful in detecting the seven faults, while basic gas ratio failed in five cases as shown in Table 8. This leads us to the conclusion that Duval method is more accurate method in detecting the faults studied in the paper. Interpreting our results, one can conclude that the accuracy of Duval makes it the promising approach in interpreting DGA results for building dependable AMS. Combining Duval with measurements and other routine tests to diagnose power transformer faults and handling multiple faults are the future course of this investigation.

ACKNOWLEDGMENT

The authors thank Dr. Shrinet, ERDA, Govt. of India, for his valuable inputs.

REFERENCES

1. M. Duval, "A review of faults detectable by gas-in-oil analysis in transformers," IEEE Electrical Insulation Magazine, 2002, 18(3), 8-17.
2. Q. Su, C. Mi, L.L. Lai and P. Austin, "A fuzzy dissolved gas analysis method for the diagnosis of multiple incipient faults in a transformer," IEEE Trans. Power Syst., vol. 15(2), pp. 593-598, 2000.
3. N.A. Muhamad, B. T. Phung, T.R. Blackburn and K.X. Lai, "Comparative study and analysis of DGA methods for transformer mineral oil," IEEE Lausanne Power Tech, pp. 45-50, July 2007.
4. D. V. S. S. Siva Sarma and G. N. S. Kalyani, "ANN approach for condition monitoring of power transformers using DGA," IEEE Region 10 Conference Vol. 100, pp. 444-447, Nov. 2004.
5. N.A. Muhamad, B. T. Phung, and T. R. Blackburn, "Comparative study and analysis of DGA methods for mineral oil using fuzzy logic," IEEE In Power Engineering Conference, pp. 1301-1306, Dec. 2007.
6. IEC Mineral oil impregnated electrical equipment in service- Guide to the interpretation of dissolved and free gas analysis, IEC Std. 60599, May 1999.
7. X. Zhang and E. Gockenbach, "Asset-management of transformers based on condition monitoring and standard diagnosis," IEEE Electrical Insulation Magazine, 24(4), 26-40, 2008.
8. A.E. Abu-Elanien and M.M.A. Salama, "Survey on the transformer condition monitoring," IEEE In Power Engineering, Large Engineering Systems Conference pp. 187-191, Oct. 2007.
9. S. Kumar, P. Shukla, Y.R. Sood and R.K. Jarial, "An experimental study to know the behavior of transformer oil on ageing," IEEE In Engineering and Systems Students Conference pp. 1-6, April 2013.
10. J. Singh, Y.R. Sood and R.K. Jarial, "Condition monitoring of power transformers-bibliography survey," IEEE Electrical Insulation Magazine, 24(3), 11-25, 2008.

Generation Expansion Planning in Tamil Nadu with High Penetration of Renewables to Limit GHG Emission

¹A.Bhuvanesh, ²S.T.Jaya Christa, ³S.Kannan

Abstract – Electrical power is one of the most important factors which decide the growth of the state like Tamil Nadu (TN) in a developing country like India. The power demand is increasing day by day. The focus of this paper is on TN state, in India, which faces severe power shortages and regular power cuts. Rapid growth in demand, high transmission & distribution losses and insufficient generation capacity are the reasons behind this problem. Seasonal change in the availability of hydropower, larger penetration of wind power, and huge dependence on imported fuel oil for power generation are the main reasons for the power shortage. This shortage of electricity has severely affected the State's as well as the nation's economy. In order to develop our country, it is necessary to overcome the issue of power shortage quickly. This paper deals with the reasons behind the present power shortage and proposes some initiatives to be taken to solve this problem. Energy conservation and effective Generation Expansion Planning are the solutions to solve these problems.

Keywords – Energy conservation, Generation Expansion Planning, Power shortage and Tamil Nadu.

I. INTRODUCTION

Electricity plays a vital role in developing the economy of the State or a Country. So, it should be generated using the local resources available in the State or the national resource of that country. The major portion of electricity generation in TN highly depends on coal, wind and water. Seasonal variation in the availability of hydro and wind power and more dependence on imported fuel such as coal, oil for power generation result in power shortage. Even though, several power generating units have been added to the grid to solve the power shortage issue, still they are not adequate. Increasing need of electric power has made a big challenge for the power system planners to meet the demand. The shortage of electricity severely hits the industrial production. The power shortages have resulted in an annual loss of about 2% of Gross Domestic Product (GDP) [1] and huge losses in total industrial production. The present power shortage is a self-imposed problem resultant from years of unskilled management, poor future vision and poor policies. According to the annual load generation balance report (LGBR) from the Central Electricity Authority (CEA), TN will face a 4.4 per cent average power deficit during 2015-16 [2]. Now, the problem has grown highly beyond any instant solution.

II.

II. PERSPECTIVE OF TAMIL NADU POWER SECTOR

TNEB was restructured on 1.11.2010 into TNEB Limited; Tamil Nadu Generation and Distribution Corporation Limited (TANGEDCO); and Tamil Nadu Transmission Corporation Limited (TANTRANSCO). According to TANGEDCO, TN has an installed capacity of 23104.91 MW, including allocated shares in joint and central sector utilities as of July 2015. The plant wise installed capacity in TN as of July 2015 is shown in Figure 1.

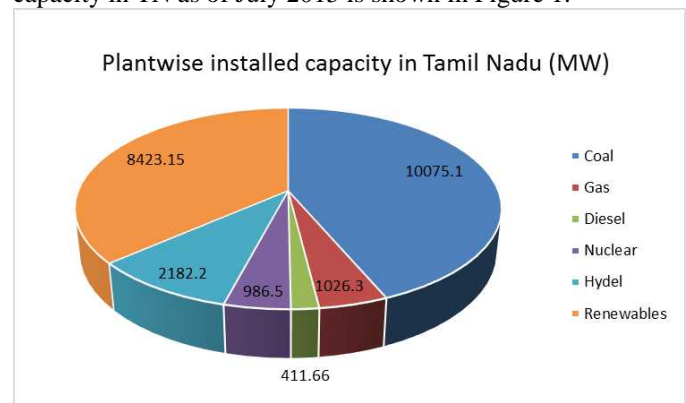


Figure 1: Plant wise installed capacity in Tamil Nadu as of July 2015

The electrical energy requirement is increasing every year at a rate of 6.65% in TN [4]. So the energy demand - supply gap in TN is also increasing. In order to avoid this

¹Research Scholar, ²Associate Professor,

^{1,2}Department of EEE, Mepco Schlenk Engineering College, Sivakasi.

³Professor & Head, Department of EEE, Ramco Institute of Technology, Rajapalayam, India.

E-mail: bhuvanesh.ananthan@gmail.com

problem, the following projects and targets are proposed to be implemented before 2023 by TN government [6].

- Building an additional 20,000 MW of power generating capacity with two Ultra Mega Power Projects of 4,000 MW each;
- Maximizing the investments in Wind Power and Solar energy to increase renewable generation capacity of 10,000 MW;
- Investing in the transmission sector to create the required evacuation capacity with buffers for the higher power generation capacity;
- Establishing two greenfield Liquefied natural gas (LNG) terminals with 5 Million Tons Per Annum (MPTA) capacity each and city gas pipeline infrastructure for 10 towns;
- Establishing smart grid system with lower cost of energy to consumers, allowing innovation in energy management at all levels in the energy chain across the economy and improving the reliability and security of the electricity grid;
- Reforming the power sector in a progressive manner to deliver reliable power to consumers at least cost.

The proposed projects / programmes in power sector of TN are given in Table 1.

TABLE 1 Proposed projects/programmes with investment cost in TN power sector [6, 7]

<i>Sector</i>	<i>Projects / Programmes</i>	<i>Investment (Rs. In Crores)</i>
Generation	North Chennai Thermal Power Project (Stage III) - 800 MW	4,800
Generation	North Chennai Thermal Power Project (Stage IV) - 1600 MW (2x800 MW)	11,155
Generation	Ennore Thermal Power station Expansion - 660 MW	3,135
Generation	Tuticorin Thermal Power Project - 800 MW	4,800
Generation	Uppur (Thiruvadana) Thermal Power Projects - 1600 MW (2x800 MW)	9,600
Generation	Udangudi Super Critical Power Project 1600 MW (2x800 MW)	9,083
Generation	Udangudi Expansion - 800 MW	4,800
Generation	Ennore Thermal Power station Replacement - 660 MW	3,600
Generation	Cheyur UMPP - 4000 MW (TN Share - 1600 MW)	19,200
Generation	New project - 800 MW	4,800
Generation	New project - 800 MW	4,800
Generation	Chattisgarh-MTMTTEL-2000 MW (TN Share-1000 MW)	4,800
Generation	Jayamkondan Lignite Power Plant (1500 MW)	6,000
Generation	Private Sector Power generation projects	10,000
Generation	R-LNG based Gas Turbine Power Plant - 1000 MW	4,000
Renewable	Small Hydro - Periyar Vaigai (5 to 17) - 30 MW	240
Renewable	Kolimalai Hydro-electric project - 20 MW	258
Renewable	Kundah Pumped Storage - 500 MW	1,500
Renewable	Sillahalla Pumped Storage HEP - 2000 MW	6,914
Renewable	Vellimalai Pumped Storage HEP (200 MW)	1,200
Renewable	Programme - Solar Power Generation (2000 MW)	50,000
Renewable	Programme - Offshore Wind Generation Programme (200 MW)	2,500
Renewable	Ministry of New & Renewable Energy (MNRE), Grid Connected Rooftop and Small Solar Power Plants Programme (100 MW)	120
Renewable	Programme - Wind Generation Programme (10000 MW)	60,000
Transmission	Identified Projects - TAN TRANSCO	16,000

Transmission	Identified Projects - CTU (PGCIL)	18,000
Transmission	Proposed Programme – TAN TRANSCO	54,000
Transmission	Proposed Programme – CTU (PGCIL)	12,000
Distribution	Distribution infrastructure - LT and HT lines and transformers	15,000
Distribution	Feeder Separation Project	16,000
Distribution	Programme - Smart Grid	20,000
Gas Grid	Development of a State Gas Grid and City Gas Networks in select cities	10,000
Solar Homes	Provision of Solar Home Lights	900
Solar Street light	Energising Street Lights with Solar Power	250
	TOTAL	389,455

The government has proposed large amount of projects in generation sector to avoid power shortage which include renewables also. If the generation expansion planning (GEP) is poor then, the power shortage will continue, though the installed capacity is higher than the peak demand. The reason for this is, 46% of electrical energy is now availed from seasonally variable renewable sources such as wind, solar and hydro. So, an efficient plan is required for generation expansion at least cost and less harmful emission to the environment. Many software tools are available for power system planning which also consider integration of renewable energy sources. A review on the different software tools that can be used to analyse the integration of renewable energy in power system planning are presented in [8]. The government needs to concentrate on actions to be taken for increasing the power conservation efforts in the state, before planning the generation expansion.

III. ELECTRICAL ENERGY CONSERVATION

Energy conservation (EC) refers using energy more efficiently or reducing the wastage of energy. The energy conservation plan aims to reduce wastage of energy without affecting productivity and growth rate. The primary objective of energy management is to increase profits and reduce costs. The main objectives of energy management programs are [9]:

- To improve energy efficiency and reduce energy use, thereby reduce the costs.
- To reduce greenhouse gas emissions and improve air quality.
- To initiate good communication on energy matters.
- To develop and maintain excellent monitoring, reporting and management strategies for wise energy usage.
- To evaluate better ways to increase returns from energy investments through research and development.
- To reduce the impacts of curtailments, brownouts or any interruption in energy supply.

A. EC in power sector

EC in power sector deals with improving energy efficiency in generation, transmission, distribution and reducing energy consumption the end user [10].

a. EC in generation side

TANGEDCO requires approximately Rs 4.5-5.25 crores to generate 1 MW of power. If the EC scenario is followed, it is able to save Rs.1 Crores/MW. The opportunity for EC in generating area is less but it can be achieved by improving the performance or efficiency of generators by optimization of load, optimal distribution of load among different units, frequent maintenance and also increasing the capacity by integrating renewable energy sources.

b. EC in transmission and distribution (T&D) side

TANTRANSCO requires approximately Rs 2 crores to transmit 1 MW of power. But the T&D system in TN has a loss of about 19% [11]. Power losses in T&D system can be classified as Technical losses and Commercial losses. Technical losses occur due to poor system planning, improper voltage and poor power factor etc. Commercial losses occur due to ineffective management, improper maintenance, corruption etc.

Metering losses occur due to inadequate billings, faulty metering, overuse and outright theft. Poor quality of the metering equipment results in metering fault. It is able to save Rs.1 Crores/MW, if the EC scenario is implemented in T&D system.

c. Demand Side Management in End-User Side

Demand Side Management (DSM) means reducing electricity usage through events that encourage electrical energy efficiency or conservation.

These activities may:

- Promote to purchase energy-efficient products.
- Promote to replace incandescent lights to more efficient lights.
- Encourage the usage of high efficient motors in industrial and domestic applications.
- Encourage customers to shift non-critical usage of electricity from peak hours to off peak hours.
- Consist of programs providing limited utility control of customer equipment such as air conditioners.
- Promote energy awareness and education.

If EC is promoted successfully in all the areas of power sector are, it will be more effective to plan about generation expansion with reduced demand.

IV. GENERATION EXPANSION PLANNING

The GEP problem consists of evaluating a perfect technology, expansion size, site and time of construction of new plants over a long planning horizon in an economic manner, guaranteeing that the installed capacity sufficiently meets the forecasted demand [12]. Also it determines WHAT type of generation plants should be constructed, WHERE and WHEN they should be committed over a long-range planning horizon [13, 14]. The basic objective of the GEP problem is to determine the least cost investment and operating plans to meet the load demand with low environmental pollution. GEP can be performed with automatic tools or by solving the GEP problem objective function [15]. A detailed description of the highly accessed tools for GEP is given in Table 2. Table 2 shows that the tools LEAP and EnergyPLAN will give better options to solve GEP than other tools. Even though, the automatic tools for GEP are simple to use and quickly provide results, the user cannot able to understand or modify the programming codes. It is necessary to understand the procedures which are followed for GEP. So GEP using MATLAB coding will be more efficient for the beginners. The GEP problem is to find a set of best decision vectors over a planning horizon that minimize the investment and operating costs, which integrates Renewable Energy Resources (RES) as to limit environment emission has been presented [3]. In this method the constraints such as construction limit, reserve margin, Fuel Mix Ratio, Reliability Criterion and Emission Constraints are all considered.

In the GEP problem formulation, the currently operating power plants and proposed power plants in TN are taken as existing and candidate plants respectively. The GEP

problem formulation is given in Appendix. It is not easy to build all the proposed power plants in a short period. The technical and economic data of existing plants and candidate plants, which can be built in the short period are given in Table A1 and Table A2 in Appendix. Optimization techniques can be applied to solve the GEP problem and to obtain the best results. The best result will provide the least cost operating combination of power plants with low emission levels affecting the environment.

V. CONCLUSION

TN power sector is affected by a number of organisational weaknesses, with inefficient generation systems, dependence on expensive fuels, financial mismanagement and poor energy policies. Efficient planning in the processes of generation expansion could be an important factor for a fair and sustainable electricity sector. Better governance will allow for planning and implementing decisions on generation expansion at the right time. A detailed discussion on power crisis and its solutions for Tamil Nadu are presented in this paper. Awareness of energy conservation will result in reduced demand of electricity. GEP can be done with the power plants which are in operating condition and under construction stage. The complete description on software tools and objective function formulation for GEP are also presented. It is concluded that the GEP with Renewable Energy Resources will provide least cost operation of power plants with low harmful emissions affecting the environment. The best solution of GEP problem will provide more benefits to Tamil Nadu power sector.

Table 2: Detailed description of the GEP tools

<i>Tool</i>	<i>Availability</i>	<i>Approach</i>	<i>Geographical area</i>	<i>Timeframe</i>	<i>Time step</i>	<i>Penetration of renewable</i>
LEAP	Commercial/free for developing countries and students	Scenario & Simulation	National/state/regional	No limit	Yearly	High
EnergyPLAN	Free to Download	Scenario & Simulation	National/state/regional	1 year	Hourly	High
WASP	Commercial/Free to IAEA member states	Simulation	National/state/regional	Max 50 years	12 load duration curves for a year	Low
EMPS	Commercial	Optimisation	International	Max 25 years	Weekly	Medium
ENPEP-BALANCE	Free to Download	Scenario	National/state/regional	Max 75 years	Yearly	Low
Mesap PlaNet	Commercial	Scenario	National/state/regional	No limit	Any	High
NEMS	Free/Simulators must be purchased	Scenario	National/state/regional	Max 50 years	Yearly	Low
RAMSES	Commercial	Simulation	International	Max 30 years	Hourly	Low
E4cast	Commercial	Scenario	National/state/regional	Max 50 years	Yearly	Low
H2RES	Internal use only	Scenario & Simulation	Island	No limit	Hourly	High
WILMAR	Commercial	Simulation	International	1 year	Hourly	High

ACKNOWLEDGMENT

The authors gratefully acknowledge the management of Mepco Schlenk Engineering College and Ramco Institute of Technology, Tamilnadu for their constant support and encouragement during this research.

REFERENCES

- [1] Abbasi Z, "Energy Crisis Costs 2 Percent of GDP Annually", Business Recorder, July 07, 2011.
- [2] www.cea.nic.in/reports/yearly/lgbr_report.pdf.
- [3] K. Rajesh, A. Bhuvanesh, S. Kannan, C. Thangaraj, "Least cost generation expansion planning with solar power plant using Differential Evolution algorithm", Elsevier Renewable Energy, vol. 85, pp. 677-686, 2016.
- [4] K.Karunanithi, S.Kannan, C.Thangaraj, "Generation Expansion Planning for Tamil Nadu- A case study", International Transactions on Electrical Energy Systems, 2014, DOI: 10.1002/etep.
- [5] Chattopadhyay, Deb, and Mohar Chattopadhyay. "Climate-aware generation planning: a case study of the Tamil Nadu power system in India." The Electricity Journal 25, no. 6 (2012): 62-78.
- [6] The Vision Tamil Nadu 2023; Strategic Plan for Infrastructure Development in Tamil Nadu, Government of Tamil Nadu, February 2014.
- [7] <http://teda.in/pdf/NOTIFICATION%20ON%20GRIDTIE%20SOLAR%20ROOF%20TOP%20POWER%20PLANT.pdf>
- [8] D. Connolly, H. Lund, B.V. Mathiesen and M. Leahy, "A review of computer tools for analyzing the integration of renewable energy into various energy systems", Elsevier Applied Energy, vol. 87, pp. 1059–1082, 2010.
- [9] Harpreet Kaur and Kamaldeep Kaur, "Energy Conservation: An effective way of energy Utilization," International Journal of Management, IT and Engineering, vol. 2, no. 5, pp. 623-37, 2012.
- [10] Nisha V.Vader and R.U.Patil, "Energy Conservation in Electrical System," In: National Conference on Recent Trends in Engineering & Technology, Vashi, 2009.
- [11] Power Sector in Tamil Nadu: A Comparative Analysis; Athena Infonomics India Pvt. Ltd, 2011.
- [12] H. M. Khodr, J.F. Gomez, L. Barnique, J. H. Vivas, P. Paiva, J. M. Yusta and A.J. Urdaneta, "A linear programming methodology for the optimization of electric power generation schemes," IEEE Transactions on Power Systems. Vol. 17, no. 3, pp. 864-869, 2002.
- [13] Wang X, McDonald JR. Modern Power System Planning. London: McGraw Hill; 1994, pp. 208-229.
- [14] Khokhar JS. Programming Models for the Electricity Industry. New Delhi, Delhi: Commonwealth Publishers; 1997, pp. 21–84.
- [15] Wang X, McDonald JR. Modern Power System Planning. London: McGraw Hill; 1994, pp. 208-229.
- [16] <http://globalenergyobservatory.org/>

APPENDIX

A. Generation Expansion Planning (GEP) Problem Formulation

The GEP problem is equivalent to finding a set of best decision vectors over a planning horizon that minimizes the investment and operating costs under relevant constraints.

A. Cost Objective

The cost objective is represented by the following expression

$$\min Cost = \sum_{t=1}^T [I(U_t) + M(X_t) + O(X_t) - S(U_t)] \quad (1)$$

where,

$$X_t = X_{t-1} + U_t \quad (t=1,2,\dots,T) \quad (2)$$

$$I(U_t) = (1+d)^{-2t} \sum_{i=1}^N (CI_i \times U_{t,i}) \quad (3)$$

$$S(U_t) = (1+d)^{-t} \sum_{i=1}^N (CI_i \times \delta_i \times U_{t,i}) \quad (4)$$

$$M(X_t) = \sum_{s=0}^1 \left((1+d)^{1.5+t+s} \left(\sum (X_t \times FC) + EC + MC \right) \right) \quad (5)$$

$$O(X_t) = EENS \times OC \times \sum_{s=0}^1 \left((1+d)^{1.5+t+s} \right) \quad (6)$$

The outage cost calculation of (6), used in (1), depends on Expected Energy Not Served (EENS). The equivalent energy function method [10] is used to calculate EENS (and also to calculate loss of load probability, LOLP, used in the constraint objective).

$$t' = 2(t-1) \quad \text{and} \quad T' = 2 \times T - t' \quad (7)$$

and

Cost total cost, \$;

U_t N-dimensional vector of introduced units in the stage t (1 stage = 2 years);

$U_{t,i}$ the number of introduced units of type i in stage t ;

X_t cumulative capacity vector of existing units in stage t , (MW);

$I(U_t)$ is the investment cost of the introduced unit at the t -th stage, \$;

$M(X_t)$ total operation and maintenance cost of existing and the newly introduced units, \$;

s' variable used to indicate that the maintenance cost is calculated at the middle of each year;

$O(X_t)$ outage cost of the existing and the introduced units, \$;

$S(U_t)$ salvage value of the introduced unit at t -th interval, \$;

d discount rate;

CI_i capital investment cost of i -th unit, \$;

δ_i salvage factor of i -th unit;

T length of the planning horizon (in stages);

N total number of different types of units;

FC fixed operation and maintenance cost of the units, \$/MW;

EC emission cost of the units, \$/MW;

MC variable operation and maintenance cost of the units, \$;

$EENS$ Expected energy not served, MWhrs;

OC value of outage cost constant, \$/MWhrs

B. Constraints

a. *Construction limit*: Let U_t represent the units to be committed in the expansion plan at stage t that must satisfy

$$0 \leq U_t \leq U_{\max,t} \quad (8)$$

where $U_{\max,t}$ is the maximum construction capacity of the units at stage t .

b. *Reserve Margin*: The selected units must satisfy the minimum and maximum reserve margin.

$$(1 + R_{\min}) \times D_t \leq \sum_{i=1}^N X_{t,i} \leq (1 + R_{\max}) \times D_t \quad (9)$$

where

- R_{\min} minimum reserve margin;
- R_{\max} maximum reserve margin;
- D_t demand at the t -th stage in megawatts (MW);
- $X_{t,i}$ cumulative capacity of i -th unit at stage t .

c. *Fuel Mix Ratio*: The GEP has different types of generating units. The selected units along with the existing units of each type must satisfy the fuel mix ratio

$$FM_{\min}^j \leq X_{t,j} / \sum_{i=1}^N X_{t,i} \leq FM_{\max}^j \quad j=1, 2, \dots, N \quad (10)$$

where

FM_{\min}^j minimum fuel mix ratio of j -th type;

FM_{\max}^j maximum fuel mix ratio of j -th type;
 j type of the unit.

d. *Reliability Criterion*: The introduced units along with the existing units must satisfy a reliability criterion on loss of load probability (LOLP)

$$LOLP(X_t) \leq \varepsilon \quad (11)$$

where ε is the reliability criterion, a fraction, for maximum allowable LOLP. Minimum reserve margin constraint avoids the need for a separate demand constraint.

e. *Emission Constraints*

The emission constraints are

$$\sum X_{t,j} e c_j < \lambda \quad (12)$$

Table A1 Technical and economic data of Candidate plants as per Vision Tamil Nadu 2023 [6]

Candidate Type	Construction Upper limit	Capacity (MW)	FOR (%)	Operating Cost (\$/kWh)	Fixed O&M Cost (\$/kw-Mon)	Capital Cost (\$/kW)	Life Time (Years)
Udangudi Thermal Power Station (UTPS)	3	800	20	0.02	3.15	3246	40
Cheyyur Ultra Mega Power Projects (CUMPP)	2	800	20	0.025	3.15	3246	40
Uppur Thermal Power Projects (UTPP)	2	800	15	0.02	3.15	3246	40
North Chennai Thermal Power Project (NCTPP)	3	800	15	0.025	3.15	3246	40
Ennore Thermal Power Station (ETPS)	2	660	20	0.02	3.15	3246	40
Jayamkondan Lignite Power Plant (JLPP)	1	1500	10	0.03	3.64	3475	40
Tuticorin Thermal Power Station-II (TTPS-II)	1	150	15	0.025	3.15	3246	40
Koodankulam Nuclear Power Plant-II (KNPP-II)	1	1000	4	0.035	7.77	5530	50
Madras Atomic Power Station-II (MAPS-II)	1	500	4	0.03	7.77	5530	50
Adani Solar	5	130	80	0.001	2.31	3873	20
Biomass	4	9	10	0.007	8.80	4114	25
Wind	5	50	70	0.002	3.29	2213	25

Table A2 Technical and economic data of existing plants in Tamil Nadu as of July 2015 [16]

Plant Type	Unit Capacity (MW)	FOR (%)	Operating Cost (\$/kWh)	Fixed O&M Cost (\$/kW-Mon)
Coal	10180	20	0.02	3.15
Gas	1023	10	0.02	1.09
Hydroelectric	2183	5	0.005	1.17
Nuclear	1000	4	0.035	7.77
Diesel	429.3	17	0.03	2.5
Wind	7948.8	70	0.002	3.29
Solar	307.98	80	0.007	2.31
Biomass	147.2	9	0.007	8.80

Electricity Generation Planning for Tamil Nadu by Considering GHG Emission Using LEAP

¹A.Bhuvanesh, ²S.T.Jaya Christa, ³S.Kannan

¹Research Scholar, ²Associate Professor,

^{1,2}Department of EEE, Mepco Schlenk Engineering College, Sivakasi

³Professor & Head, Department of EEE, Ramco Institute of Technology, Rajapalayam
E-mail: bhuvanesh.ananthan@gmail.com

Abstract. This paper presents an application of Long-Range Energy Alternative Planning (LEAP) software to investigate a range of various technologies for generating electricity at least cost for Tamil Nadu. The cost of generating electricity includes the capital, fuel, operation and maintenance costs for those technologies that are considered. Detailed analyses are performed with and without the inclusion of externality costs of local air pollution in order to examine the cheapest option of electricity generation. The impact of imposing Green House Gases (GHG) emission limit on the change in generating technologies was analyzed, considering least cost of electricity generation. Moreover, the corresponding overall cost of electricity generation was found for each case. The LEAP model to estimate least cost Electricity Generation for Tamil Nadu is proposed. The electricity generation is predicted for future years until 2025, keeping 2015 as base year. This model can be further used for predictive electricity generation after 2025 also.

Keywords. GHG Emissions, Externality costs, LEAP, least cost Electricity Generation and Tamil Nadu.

1 Introduction

Electricity plays an important role for the development of any country. It was reported that southern region of India had the highest peak demand and electrical energy shortage in 2013. Tamil Nadu, one of the states in southern region of India, had an average electrical energy shortage of 10.5 % in 2013. In the last few years Tamil Nadu is facing huge electrical energy shortage due to several reasons [1]. This problem of electrical energy shortage is being felt mainly by the industries, leading to a loss in production efficiency and heavy loss of income. This electrical energy shortage should be removed, because electrical energy is most important for socioeconomic development, particularly in the developing countries. In this era of globalization, a quick increase in urbanization, population and the energy demand show that electrical energy shortage will be the major problem in the developing countries as well as in the world in the coming years. Therefore, the electrical energy generation forecasting should be done effectively and economically. The first developed energy supply models were established on only one feature of the problem namely costs, environmental impacts, or energy supply security. The old energy supply models only reflect one energy sector or even one energy carrier.

They were developed based on econometric methods and they relate energy demand with some macroeconomic indicators such as Gross Domestic Product (GDP). Because those models were not able to take into consideration two differing goals of using low-cost electrical energy production and environment conservation, they did not have sufficient efficiency in facing the recent energy concerns [2].

In recent years, a great number of wide-ranging energy models have been developed which consider not only all energy consumption sectors and energy carriers, but also environmental aspects and the trend of energy utility's efficiency. LEAP has a significant impact in shaping energy and environmental policies worldwide. It had been successfully used in more than 150 countries worldwide for different purposes. For example, in California, (2001) LEAP was used for energy forecasting and identifying alternative fuels [3]. In Mexico, it was used to determine the feasibility of future scenarios based on moderate and high use of biofuels in the transportation and electricity generation sectors [4]. In Lebanon, mitigation options were assessed to reduce emissions from electricity generation with emphasis on the usage of renewable energy resources [5]. The energy consumption and various types of emissions in consumption sectors in Iran were analyzed by using LEAP model [6]. So far, for Tamil Nadu, an energy model of electricity is proposed using Energy and Power Evaluation Program (ENPEP-BALANCE) tool, with consideration of different RETs (Renewable Energy Technologies) for 30 years from 2013 to 2042 [7]. The various factors such as average capacity, Energy Not Served (ENS), energy consumption by demand sectors, ratio of supply and demand, average cost of energy generation, pollutants CO₂, SO₂ and Particulate Matter (PM) emitted by thermal plants are evaluated [7]. It is necessary to plan an economic future electricity generation method with low emission of GHG by concentrating the renewable energy sources (RES). The modeling studies carried out to demonstrate the impact of bringing in solar plants into the generating system as a technology alternative power plant is presented in [8]. Hence, in this paper, the application of LEAP software to investigate a range of various technologies for generating electricity in Tamil Nadu for two different cases namely single-technology simulation scenarios and optimization scenario is presented.

2 Leap and Its Features

Future prediction of electricity generation through various technologies is a challenging task. To assist the Power System Planning Engineer in this task, various tools are developed. LEAP is one such energy-planning tool developed by the Stockholm Environment Institute, Boston (SEI-B). It consists of an EDB (Environmental Database), which was also developed by SEI-B with additional support from the United Nations Environment Programme (UNEP), and is a joint UNEP/SEI activity [9]. LEAP is an accounting framework, within which the user can develop models of demand and supply. It is a long-term integrating and modelling tool. The LEAP model requires data for at least the base year and any of the future years. Then, using the function such as interpolation or extrapolation or the growth rate method, the future energy demand and emissions are

predictable for the other years. The fundamental concept in LEAP is an end-use driven scenario analysis [10].

LEAP model is mostly used for energy and environmental planning for both medium and long-term consideration. LEAP works with an unlimited time horizon with an annual time setup that can be extended up to 50 years. Different modeling approaches used by LEAP cover both the demand and supply side of energy. To model electricity generation planning and generation capacity expansion, LEAP offers a series of methodologies accompanied with accounting and simulation [11].

3 LEAP Model for Tamil Nadu

The LEAP model is developed for Tamil Nadu and the electricity is set as the only demand. The electricity can be generated by the plants namely Natural Gas (NGCC), RES, Coal, Hydro, Nuclear and Diesel. In addition, they are entered into the Process branch of LEAP model. The Carbon emitting substances to the environment are entered into the Effects branch of LEAP model.

The LEAP model for Tamil Nadu has been developed by setting the base values shown in Table 1. The model has been developed for the base year 2015 and extrapolated until 2025. The electricity demand for the year 2025 will be 200 Thousand GWh and it is one of the inputs for LEAP [7]. The electricity losses are taken as 18% for developing the model [12].

This data for various electricity generation technologies is taken from [13], [14] and [15] for January 2015. These data are entered into the Transformation module called Electricity Generation in the LEAP model, which include various electricity generation plants namely Coal, Gas, Diesel, Nuclear, Hydro and Renewable Energy Sources (RES) and its properties are fixed to Capital cost, Fixed Operation and Maintenance (OM) Cost, Variable OM Cost, Fuel cost, Capacity, Efficiency, Maximum availability, Capacity credit, Life time, system load curve and a planning reserve margin. The discount rate is set as 5% while entering the cost data.

Table 1. The Base Values of LEAP for The Year 2015 Including Various Electricity Generation Technologies

Name of the plant	Capacity (MW)	Efficiency (%)	Maximum availability (%)	Capacity credit (%)	Capital cost ($\times 10^3$ \$/MW)	Fixed OM Cost (\$/MW)	Variable OM Cost (\$/MW)	Fuel Cost (\$/MWh)	Life Time (years)
Coal	9688.10	35	90	90	2934	31.18	4.47	95.6	40
Gas	1026.30	38	90	90	917	13.17	3.60	75.8	40
Diesel	411.66	40	90	90	950	30	3.10	85	40

Nuclear	986.50	35	80	90	5530	93.28	2.14	96.1	50
Hydro	2182.20	90	90	50	2936	14.13	0	84.5	50
RES	8075.38	25	100	25	3000	52.00	0	100	50

4 Result and Discussions

The fossil fuels are expected to unavailable in 50 more years if the consumption rate remains to grow at high rate. With the unstable nature of international crude prices, it is important to reduce this dependence and look for alternatives. Therefore, the renewable energy technologies also be expanded to supply secure electrical energy at least cost and low GHG emission. The developed LEAP model for Tamil Nadu having two different cases namely Single-technology simulation scenario and Optimization scenario. In Single-technology simulation scenario the LEAP having various electricity generation technologies namely Coal Only, Diesel Only, Hydro Only, Natural Gas Only, RES Only and Nuclear Only. LEAP decides the types of power plants to be added and when to be added to meet out the demand by giving more preference to a single generation technology, based on its availability and fuel cost. The Optimization scenario is simulated to explore least cost electricity generation by considering GHG emission limit also.

4.1 Case 1: Single-Technology Simulation Scenario

In this case, a simple scenario using each of single generation technology have been simulated. They are namely, Coal only, Diesel only, Hydro only, Natural Gas only, RES only and Nuclear only. In the Coal only technology, LEAP automatically gives more preference to coal plant for generating electricity to meet out the electricity demand based on its availability. If the coal is not sufficient to generate the required electrical energy, then other sources for generating electrical energy are considered based on its fuel cost. Based on standard simulation calculations, LEAP decides the types of power plants to be added and when to be added to meet out electrical energy demand. This simulation is also carried out for all the other single generation technologies such as Diesel only, Hydro only, Natural Gas only, RES only and Nuclear only. The predicted values of capacity, Electrical energy output and Social cost in the year 2025 for various single technologies are shown in figures 1, 2 and 3 respectively.

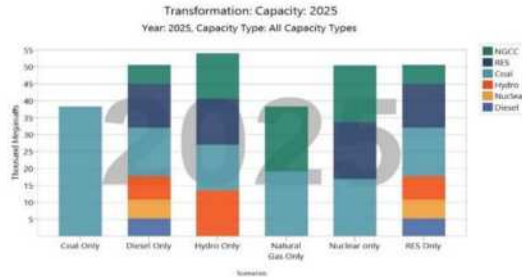


Fig. 1. Capacity values predicted by LEAP by single-technology simulation scenarios for the year 2025

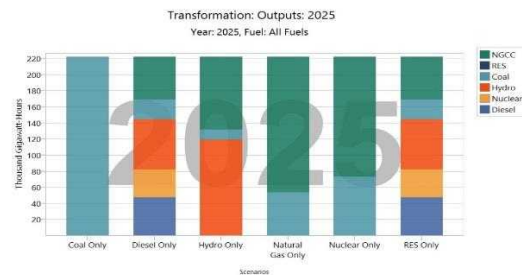


Fig. 2. Electrical Energy Output predicted by LEAP by single-technology simulation scenarios for the year 2025

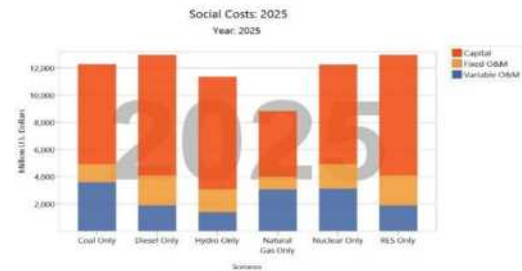


Fig. 3. Social Cost predicted by LEAP by single-technology simulation scenarios for the year 2025

The results from LEAP model show that for most of the single-technology simulation scenarios, Natural Gas technology is used to generate more amount of electrical energy and is shown in Figure 2. Figure 3 shows that the Natural Gas only generation technology will be the cheapest option for power generation in the year 2025, due to their low fuel cost.

4.2 Case 2: Optimization Scenario

The Optimization scenario allows LEAP to decide the combination of power plants which will meet demand at the lowest cost and lowest emission of GHG.

Evaluation of Least Cost Electricity Generation.

The LEAP model runs the OSeMOSYS optimization model, which is used to simulate the optimization scenario. The comparison of capacity, electrical energy output and social cost in the year 2025 using single-technology simulation scenarios and Optimization Scenario are shown in figures 4, 5 and 6 respectively.

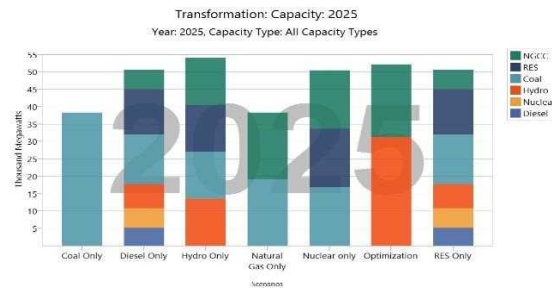


Fig. 4. Comparison of Capacity by single-technology simulation scenarios and Optimization Scenario predicted by LEAP for the year 2025

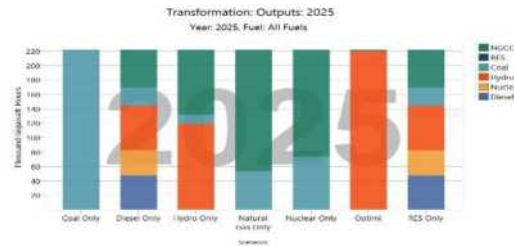


Fig. 5. Comparison of Electrical Energy Output by single-technology simulation scenarios and Optimization Scenario predicted by LEAP for the year 2025

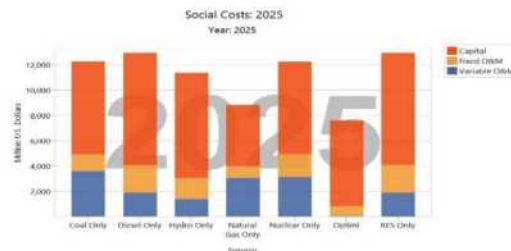


Fig. 6. Comparison of Social Cost by single-technology simulation scenarios and Optimization Scenario predicted by LEAP for the year 2025

Figure 5 shows that the LEAP has chosen a mix of power plants in the Optimization scenario, unlike the other single-technology simulation scenarios. The results show that peak load periods favor Natural Gas power plants that are relatively cheap to build but expensive to operate. Base load periods favor Hydro power plants that have higher capital cost but with low running costs. Figure 6 shows that, because of the low variable and fixed O&M cost, the total social costs of Optimization Scenario are slightly cheaper than even the cheapest of the other single-technology simulation scenarios which were created previously.

All the single-technology scenarios having maximum penetration of non-renewables in its fuel mix. So the fixed and variable O&M cost will be high. But the Optimization scenario penetrates renewables in more amount. So the fixed and variable O&M cost will be very low. So the overall cost will be minimum. The Optimization Scenario also shows a maximum level of GHG emissions is imposed on the system with least cost. The comparison of total GHG emission for generating electrical energy by single-technology simulation scenarios and Optimization Scenario predicted by LEAP for the year 2025 is shown in Figure 7.

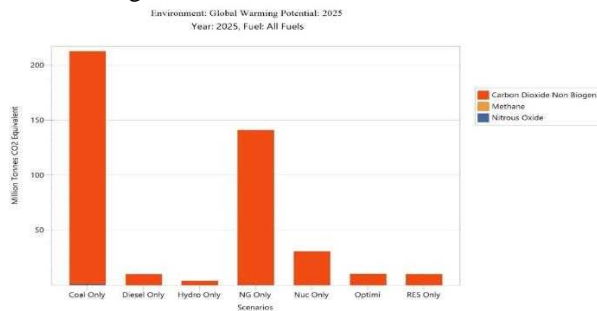


Fig. 7. Comparison of Total GHG Emission by single-technology simulation scenarios and Optimization Scenario predicted by LEAP for the year 2025

Figure 7 shows that the emission of GHG is less in Optimization Scenario next to Hydro Only single-technology simulation scenario, compared to other single-technology simulation scenarios.

5 Conclusion

The application of Long-Range Energy Alternative Planning (LEAP) software to investigate a range of various technologies for generating electricity, at least cost for Tamil Nadu is presented in this paper. The LEAP model was developed to estimate least cost Electric Generation by considering GHG emission factor for Tamil Nadu for the base year 2015 and extrapolated till 2025 for the future generation expansion planning. The LEAP model was developed for two different cases such as single-technology simulation scenario and optimization scenario. The predicted electrical energy output and social cost

values are obtained for the two cases. The results show that the optimization scenario gives the least cost generating capability to meet the demand with less emission of GHG.

References

- [1] S.R.Rallapalli, S. Ghosh.: Forecasting monthly peak demand of electricity in India-A critique. *Energy Policy*, vol. 45. (2012) 516-520.
- [2] M.A. Moradi, H. Shakouri, A.M. Aboutaleb.: Developing the Electricity Demand Model for Iran's Residential Sector; Based on LEAP. *International Power System Conference*, Tehran, Iran, (2013).
- [3] Ghanadan, R., J.G. Koomey.: Using energy scenarios to explore alternative energy pathways in California. *Energy Policy*, vol. 33. (2005) 1117-1142.
- [4] Islasa, J., F. Manzini., O. Masera.: A prospective study of bioenergy use in Mexico. *Energy*, vol. 32. (2007) 2306-2320.
- [5] El-Fadel, M., M. Zeinati, N. Ghaddar., T. Mezher.: Mitigating energy-related GHG emissions through renewable energy. *Energy Policy*, vol. 29. (2001) 1031-1043.
- [6] Awami, A., B. Farahmandpour.: Analysis of environmental emissions and greenhouse gases in Islamic Republic of Iran. *International Institute for Energy Studies*, vol. 4. (2008).
- [7] B.R.Prabakar, K.Karunanithi, S.Kannan, C. Thangaraj.: Energy Model of Electric Sector for Tamil Nadu. *International Journal of Applied Engineering Research*, vol. 10. (2015) 5681-87.
- [8] K. Rajesh, A. Bhuvanesh, S. Kannan, C. Thangaraj.: Least cost generation expansion planning with solar power plant using Differential Evolution algorithm. *Elsevier Renewable Energy*, vol. 85. (2016) 677-686.
- [9] Long range energy alternatives planning system. Boston. SEI-Stockholm Environment Institute, Tellus Institute, (2008).
- [10] Rabia Shabbir., Sheikh Saeed Ahmad.: Monitoring urban transport air pollution and energy demand in Rawalpindi and Islamabad using leap model. *Elsevier Energy*, vol. 35. (2010) 2323-2332.
- [11] Syeda Shaima Meryem, Sheikh Saeed Ahmad, Neelam Aziz.: Evaluation of biomass potential for renewable energy in Pakistan using LEAP model. *International Journal of Emerging Trends in Engineering and Development*, vol.1. (2013) 243-249.
- [12] Power Sector in Tamil Nadu: A Comparative Analysis. Athena Infonomics India Pvt. Ltd, (2011).
- [13] Executive Summary Power Sector. Government of India Ministry of Power Central Electricity Authority New Delhi, (2015).
- [14] Annual Energy Outlook. U.S. Energy Information Administration, (2015).
- [15] Updated Capital Cost Estimates for Utility Scale Electricity Generating Plants. U.S. Energy Information Administration, (2013).

Power Quality Enhancement Employing Genetic Algorithm based Asymmetrical Multilevel Inverter

S.Suresh, S.Kannan and B.V.Manikandan

Abstract—This paper presents the performance and power quality analysis of Asymmetrical Cascaded Multilevel Inverter in terms of various parameters like voltage, current and Total Harmonic Distortion. Simulations of Asymmetrical Cascaded Multilevel Inverter are performed and analyzed for different levels of output voltages with harmonic profile. Genetic Algorithm is used to find out the switching angles at fundamental frequency through optimized harmonic elimination technique. From simulation and experimental results, Genetic Algorithm has improved the harmonic profile of voltage and current for various possible Modulation Index values. Experimental results are compared with the simulation results for showing reduction of lower order harmonics after applying Genetic Algorithm based switching angles. Improvement has been achieved in voltage and current waveform. Total Harmonic Distortion and switching losses have been measured for various Modulation Index values.

Index Terms—Genetic Algorithm, Power Quality, Static Power Converters, Switching Loss and Total Harmonic Distortion

I. INTRODUCTION

POWER Quality (PQ) issues bring more attention towards Industry applications, utility development and various consumer loads. The harmonic trouble occurs in industries because of the usage of variable speed drives. Further, the harmonics happen in the utility services, due to the interconnection and coupling between the power electronic based micro grid. The reactive power demand, the voltage fluctuations and the unbalanced current result in serious problems in power distribution systems. i.e., increased line losses, decreased power transmission capacity, decreased stability of power system, decreased/increased system voltage, harmonic injection, etc.

Researchers get attracted towards Multi Level Inverters because of its varied topology, high power conversion ability with improved PQ, sinusoidal like output voltage and the direct high voltage transmission system inter-link facility with small DC power sources. The multilevel inverter concepts were developed three decades ago [1]-[5]. Multilevel inverter applications are extended for real power control, reactive power control, and harmonic mitigation in the existing power distribution system. The cascaded multilevel inverters are mainly classified as Symmetrical Cascaded Multi Level Inverter (SCMLI) and Asymmetrical Cascaded Multi Level Inverter (ACMLI). The SCMLI processes equal DC voltage sources, whereas ACMLI processes unequal DC voltage sources with less number of switches, for the same levels of stepped AC voltage. The ACMLI comprises differently rated power semiconductor devices (hybrid) for the construction of individual H-bridge inverter with different capacities and different switching frequencies. However, the synthesized output voltage frequency is fundamental [6]-[9]. The number of components used in the topology of ACMLI has been reduced, which simplifies the control system and enables low cost hardware implementation. Recently, so many topologies have been proposed to reduce the involvement of number of switches and therefore, low switching losses occur for generating the same number of steps in the output voltage [10]-[13]. Cascaded sub-multilevel inverter topology has been discussed for the operation of both SCMLI and ACMLI [14]-[15]. Various harmonics reduction techniques have been applied for PQ improvement. However, the solution could not be obtained for all values of Modulation Index (MI) [16]-[18]. Soft computing techniques are being used for control and PQ improvement in multilevel inverter. Genetic Algorithm (GA) is used to minimize the lower order harmonics by solving the fundamental equations of inverter obtained from Fourier series analysis [19]-[20].

In this paper, an improved GA has been proposed to find out the switching angles in order to minimize the lower order harmonics in the output voltage and to improve the quality of waveform. The ACMLI consisting of 2 bridges per phase and 3 bridges per phase has been considered and the outputs are presented. This paper is organized as follows: Section 2 illustrates the configuration and the operation of ACMLI. Section 3 presents the analysis and control of inverter. Section

S.Suresh is the Research Scholar, Kalasalingam University, Anand Nagar, Krishnankoil, Tamil Nadu, 626126, India (e-mail: sureshped07@gmail.com).

S.Kannan, is Prof & HoD of Electrical & Electronics Engineering Dept., Ramco Institute of Technology, Rajapalayam, Tamil Nadu, 626117, India (e-mail: kannaneeeps@gmail.com).

B.V.Manikandan is the Asso. Prof of Electrical Engineering Department, MepcoSchlenk Engineering College, Sivakasi, Tamil Nadu, 626005, India (e-mail: bvmani73@yahoo.com).

4 depicts the role of GA in harmonic reduction. Section 5 describes the simulation and experimental results with discussions and Section 6 gives the conclusions of the proposed method.

II. INVERTER CONFIGURATION AND OPERATION

The three-phase circuit diagram of seventeen levels ACMLI is shown in Fig.1. In this diagram, the supply voltage in the input side can be fixed as a binary or ternary ratio (for getting expected number of steps in output voltage with almost closest to sinusoidal waveform, which enhances the PQ). Table I shows the calculation of number of levels/steps in the output voltage for single phase and three-phase systems for specified number of H-bridge inverter units built in SCMLI and ACMLI topologies. In SCMLI topology, all H-bridge inverter units have equal voltage V_{dc} , the total input dc voltage is equal to the multiplication of number of H-Bridge inverter units and the voltage ($n*V_{dc}$). In ACMLI topology, the H-Bridge inverter unit has unequal voltage sharing, determined by binary/ternary term and the term N uses to find out the total input dc voltage sources using the term S depending upon the binary/ternary term.

$$N = \sum_{s=0}^{n-1} 2^s = \sum_{s=0}^{n-1} 3^s$$

TABLE I
CALCULATION OF VOLTAGE LEVELS FROM NUMBER OF BRIDGES

Number of H-Bridges (n)	Symmetric Cascaded Multi Level inverter (SCMLI)		Asymmetric Cascaded Multi Level Inverter (ACMLI)	
	Single phase (2n+1)	Three Phase (4n+1)	Single phase (2N+1)	Three Phase (4N+1)
1	3	5	3/3	5/5
2	5	9	7/9	13/17
3	7	13	15/27	29/53

Table II shows the calculation of number of steps in output voltage waveform for different inputs.

TABLE II
NUMBER OF H-BRIDGES AND OUTPUT VOLTAGE LEVELS IN BINARY AND TERNARY TERM INPUT VOLTAGE

Number of H-Bridges (n)	Asymmetric Cascaded Multi Level Inverter (ACMLI)					
	Binary inputs (P=2 ⁰ , 2 ¹ , 2 ² , ...)			Ternary inputs (P=3 ⁰ , 3 ¹ , 3 ² , ...)		
	Total Input Voltage (n)	Single phase (2n+1)	Three phase (4n+1)	Total Input voltage (n)	Single phase (2n+1)	Three phase (4n+1)
	1	V _{dc}	3	5	V _{dc}	3
2	3V _{dc}	7	13	4V _{dc}	9	17
3	7V _{dc}	15	29	13V _{dc}	27	53

In Fig.1, three single-phase inverters are connected in star configuration to implement three-phase inverter. The three-phase seventeen level ACMLI consists of two H-bridges connected in series per phase and each has different magnitudes of DC voltage in the input side. In ACMLI, the DC voltage magnitude is in multiples of two or three i.e., ([1:2:4], [1:3:9]). The switching losses are less in this topology. In this work, three phase seventeen level ACMLI topology has been presented with laboratory prototype result and the input DC voltage magnitude in each phase is taken in the ratio of 1:3. With less number of H-bridge units, it becomes possible to obtain more number of voltage levels at fundamental frequency. Table III shows the determination of level of output (stepped) voltage in one phase for various switching combinations of concerned H-bridge inverter unit.

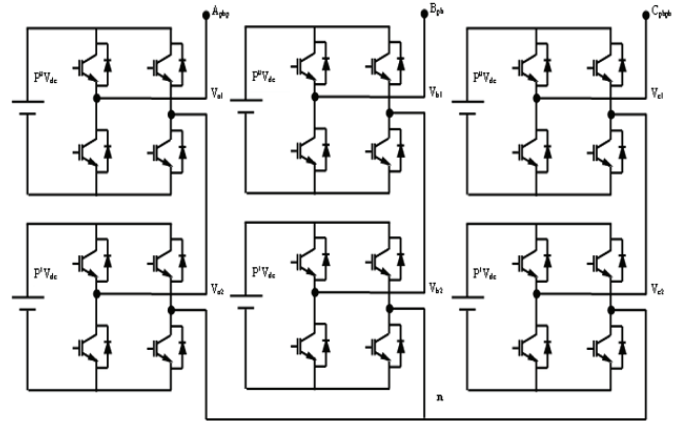


Fig1. Circuit diagram for three phase seventeen level asymmetrical cascaded multilevel inverter topology

In Table III, +1 represents $+V_{dc}$, -1 represents $-V_{dc}$ and 0 represents 0 V_{dc} of concerned H-bridge inverter. For one quarter cycle of output per phase, the switching function has been given with output voltage level in one phase of inverter. For example, the H-bridge inverters in one phase have input DC voltage of magnitude V_{dc} and $3V_{dc}$, respectively. To obtain $4V_{dc}$ magnitude in output voltage per phase, the contribution a of switching function in each inverter unit is that the phase is

TABLE III
OUTPUT VOLTAGE OF EACH H-BRIDGE INVERTER AND OUTPUT VOLTAGE (PER PHASE) LEVEL FOR TERNARY INPUT VOLTAGE TERMS

H-Bridge-1	H-Bridge-2	Output voltage(per phase) level
		9 level
V _{dc}	3V _{dc}	v _o
0	0	0
+1	0	1
-1	+1	2
0	+1	3
+1	+1	4
0	+1	3
-1	+1	2
+1	0	1
0	0	0

+1, +1 respectively. i.e, $V_{dc}+3V_{dc}=4V_{dc}$. The first inverter unit, which has input DC voltage of V_{dc} , is switched on and the second inverter unit with input DC voltage of $3V_{dc}$ is switched

on at this switching interval. All the H-bridges are connected in series to obtain this $4V_{dc}$ as peak voltage.

The inverter can produce variable AC voltage for i) variable (Modulation Index) MI with constant DC input voltage or ii) variable DC input voltage with fixed MI. Variable AC voltage for variable MI with fixed DC voltage is discussed in this paper. Variable MI method enables to make the required output voltage from fixed input dc voltage for grid applications. Because, variable MI enhances the control of reactive power and real power exchange from inverter to grid side by adjusting the inverter voltage magnitude and phase angle with respect to grid voltage.

The MATLAB/Simulink implementation of ACMLI for one phase of three-phase seventeen levels and fifty three levels has been shown in Fig.2. The output voltage for each H-bridge inverter unit and output voltage per phase are presented in Fig.3 for three-phase seventeen levels ACMLI. Fig.4 shows the output voltage for each H-bridge inverter unit and output voltage per phase for three-phase fifty-three level ACMLI. In this work, for three-phase seventeen levels, GA based switching algorithm is used to control the fundamental order voltage and to minimize the lower order voltage harmonics. For three-phase fifty-three level, a simple switching (random) determination method is used.

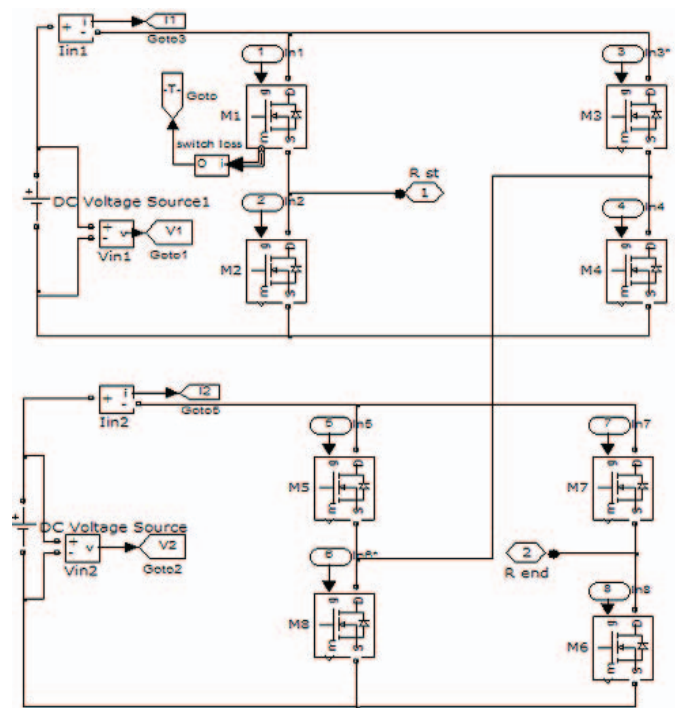


Fig 2(a). Simulation Diagram of three-phase ACMLI 17 level

From Fig.3 and Fig.4, it is understood that each H-bridge inverter unit in one phase is operated at multiples of fundamental frequency to achieve the output voltage at fundamental frequency. This enhances moderate switching loss. When the number of levels increases above certain limit, it is difficult to compute the switching time for all switches. Fig.5 shows the gating signal generation using digital logic for

pre-calculated conduction angles at different values of MI. The conduction angles have been selected randomly and

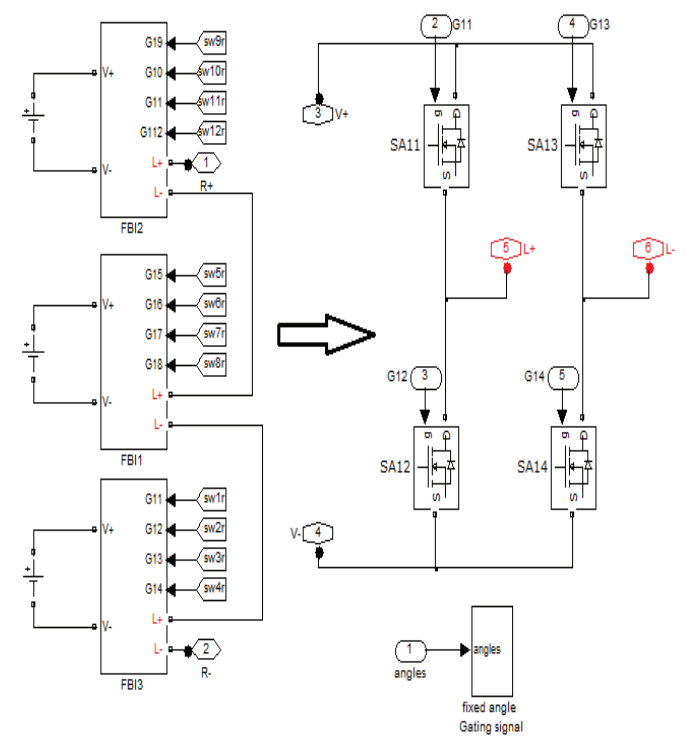


Fig 2(b). Simulation Diagram of three-phase ACMLI 53 level

calculated using GA to optimize Total Harmonic Distortion (THD) at different MI values using selective harmonic reduction technique. Using these conduction angles, gating signals are generated to operate the inverter and output voltage is generated. The randomly selected conduction angles provide no guarantee in reduction/elimination of particular

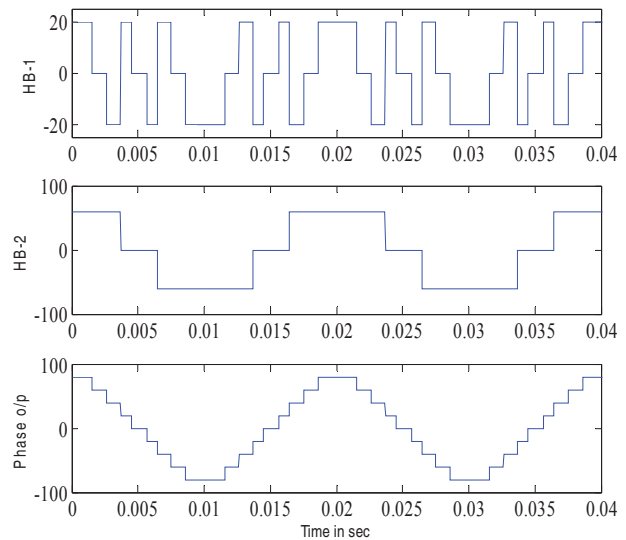


Fig 3. Output voltage of each H-bridge inverter unit and per phase voltage of three-phase 17 levels

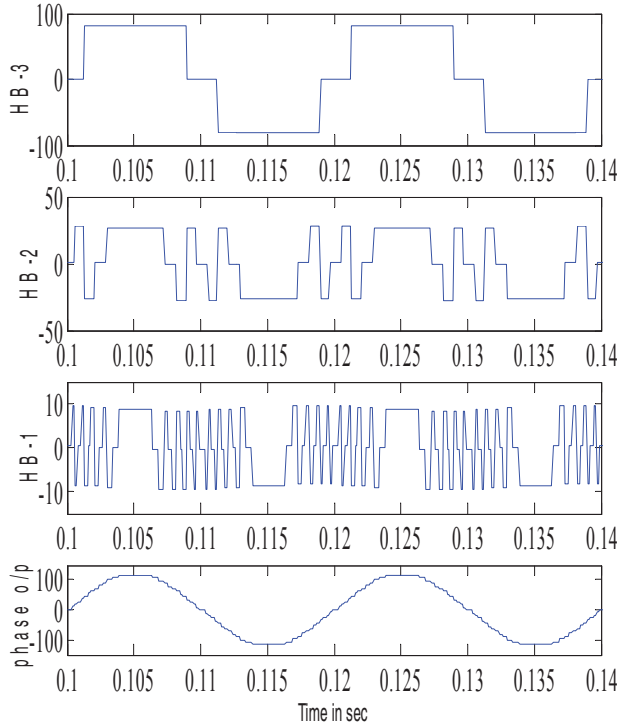


Fig 4. Output voltage of each H-bridge inverter unit and phase voltage of three-phase 53 levels

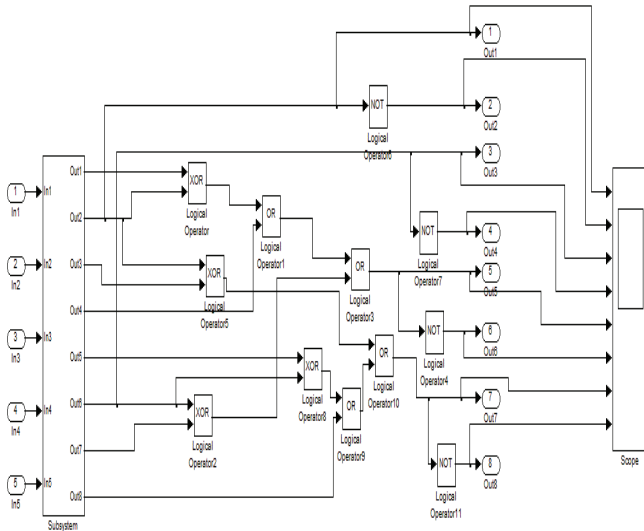


Fig 5. Simulation diagram for gating signal generation for one phase of 17 levels ACMLI using digital logic

odd harmonic value, however reduces overall THD. But, the calculated/GA optimized harmonic reduction/elimination technique guarantees elimination/reduction of specific lower order harmonic. Further, it reduces overall THD and improves PQ.

III. ANALYSIS AND CONTROL OF INVERTER

Several methods have been discussed for dq control of inverter for separate control of real power and reactive power.

The Synchronous Reference Frame (SRF) transformation is used to separate real and reactive current components. The dq values of inverter current give the details about real and reactive power components.

$$\begin{bmatrix} V_{\alpha} \\ V_{\beta} \end{bmatrix} = \frac{\sqrt{2}}{\sqrt{3}} \begin{bmatrix} 1 & -\frac{1}{2} & -\frac{1}{2} \\ 0 & \frac{\sqrt{3}}{2} & -\frac{\sqrt{3}}{2} \end{bmatrix} \begin{bmatrix} V_a \\ V_b \\ V_c \end{bmatrix} \quad (1)$$

After calculation of $\alpha\beta$ plane parameters stated in equation (1), the dq values are calculated using (2),

$$\begin{bmatrix} V_d \\ V_q \end{bmatrix} = \begin{bmatrix} \cos\theta & \sin\theta \\ -\sin\theta & \cos\theta \end{bmatrix} \begin{bmatrix} V_{\alpha} \\ V_{\beta} \end{bmatrix} \quad (2)$$

Current is also converted into dq components. The inverter can be synchronized for utility applications to supply only real power (P_i) or reactive power (Q_i) by fixing the dq axis active/reactive reference current using (3) and (4),

$$P_i = 3V_{sph}I_{sph} \sin\theta = V_{sd}I_{sd} \quad (3)$$

$$Q_i = 3V_{sph}I_{sph} \cos\theta = V_{sq}I_{sq} \quad (4)$$

Where V_{sph} and I_{sph} are inverter per phase voltage and current (RMS value), respectively.

θ is the phase angle between these voltage and current.

TABLE IV
SYSTEM PARAMETERS FOR CASE STUDY

Inverter parameters	Values of parameters
Inverter phase voltage, V_{sph}	55V RMS
Output frequency, f	50 Hz
Power rating, VA	500 VA (approx.)
Current rating, I_{inv}	10 A
Load Parameters R L	60 Ω , 36mH and 60 Ω , 60mH

V_{sd} and I_{sq} are dq components of inverter voltage and current.

A simple three-phase system has been taken for study. The per phase system parameters are given in Table IV. The inverter is designed for 500 VA capacities. Simulation studies using MATLAB/Simulink along with the detailed validation of experimental results are furnished. The inverter performance is analyzed for various MI values and the results are discussed.

IV. IMPLEMENTATION OF GENETIC ALGORITHM

Optimization problem is solved by GA, which is a computational model that solves by imitating genetic processes and the theory of evolution. It imitates biological evolution by using genetic operators such as reproduction, crossover, mutation, etc. GA finds a solution of function $f(x_1, x_2, x_3, \dots, x_k)$ using minimization/maximization and each x_i is coded as a binary or floating point string of length m shown in (5). In this work, four switching angle variables have been taken for implementing calculation of three-phase ACMLI (seventeen levels) [19]-[20]. In this analysis, a binary string is preferred. Considering

$$\begin{aligned}
 x_1 &\equiv [1010011010] \\
 x_2 &\equiv [0100101001] \\
 &\dots\dots\dots \\
 x_k &\equiv [0011010001]
 \end{aligned} \quad (5)$$

The set $\{x_1, x_2, x_3 \dots x_k\}$ is called as a solution and x_i is corresponding binary string for switching angle θ_i .

Process for GA methodology is the same for any problem. Only few parameters are needed to set a GA to work properly. The steps for applying GA to find the optimum values of switching angles are as follows:

- 1) Select binary or floating point strings.
- 2) Find the number of variables specific to the problem. In this application, the number of variables is the number of controllable switching angles. In a three-phase seventeen level inverter, it requires four voltage levels per phase, thus, each solution for this application will have four switching angles, i.e., $\{\theta_1, \theta_2, \theta_3 \& \theta_4\}$.

- 3) Set a population size and initialize the population. Higher population might increase the rate of convergence, but it also increases the execution time. In this work, the population has been taken as 100, each containing four switching angles. The population is initialized with random angles between 0° and 90° by taking into consideration the quarter-wave symmetry of the output voltage waveform.

- 4) GA has to evaluate the fitness of each solution which is the cost function. Since, the objective of this study is to minimize the specified harmonics, the cost function has to be related to these harmonics. As an example, assume that the 5th, 7th and 11th harmonics at the output of a three phase seventeen-level inverter are to be minimized with the control of fundamental component.

The transcendental equations are

$$\begin{aligned}
 V_1 &\equiv (4V_{dc}/\pi)[\cos \theta_1 + \cos \theta_2 + \cos \theta_3 + \cos \theta_4] \\
 V_5 &\equiv (4V_{dc}/5\pi)[\cos 5\theta_1 + \cos 5\theta_2 + \cos 5\theta_3 + \cos 5\theta_4] \leq 0.0001 \\
 V_7 &\equiv (4V_{dc}/7\pi)[\cos 7\theta_1 + \cos 7\theta_2 + \cos 7\theta_3 + \cos 7\theta_4] \leq 0.0001 \\
 V_{11} &\equiv (4V_{dc}/11\pi)[\cos 11\theta_1 + \cos 11\theta_2 + \cos 11\theta_3 + \cos 11\theta_4] \leq 0.0001
 \end{aligned} \quad (6)$$

The condition for angle assumption is initially $0^\circ \leq \theta_1 \leq \theta_2 \leq \theta_3 \leq \theta_4 \leq 90^\circ$

Then, the cost function can be selected as the sum of these three harmonics normalized to the fundamental,

$$f(\theta_1, \theta_2, \theta_3, \theta_4) \equiv 100(V_5 + V_7 + V_{11})/V_1 \quad (7)$$

Typically, the GA algorithm is used to solve maximization problem rather than a minimization problem. In case, where minimization is required, the negative or the reciprocal of the function to be optimized, is used. Using this formulation, the fitness value is calculated for each solution using

$$FV \equiv -100(|V_5| + |V_7| + |V_{11}|)/|V_1| \quad (8)$$

The switching angle set producing the minimum Fitness Value (FV) is the best solution of the first iteration.

- 5) The GA is usually set to run for certain number of iterations (1000 in this case) to find an optimal solution. After the first iteration, FVs are used to determine new off spring. These off-springs go through crossover and mutation

operations and a new population is created which goes through the same cycle several times. Fig.6 shows the FV obtained for the value of MI = 0.839 and the angles obtained from GA are 5.63° , 19.88° , 28.76° and 55.07° . These angles are used in hardware set up for getting the output voltage of inverter.

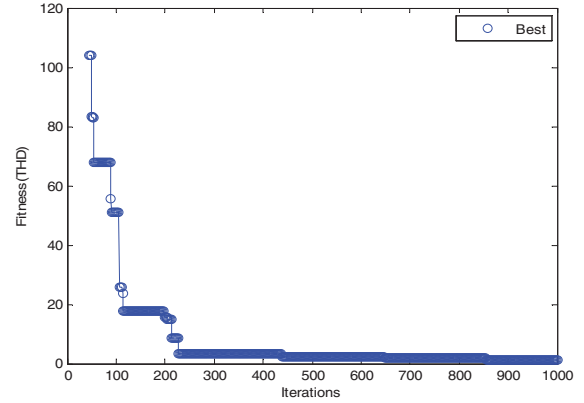


Fig 6. GA based fitness value calculation for MI = 0.839

V. RESULTS AND DISCUSSIONS

The three-phase ACMLI (seventeen and fifty-three level), along with the control block is modeled and simulation is done using MATLAB/SIMULINK. The source parameters per phase are given in Table IV. The simulation is carried out for various load conditions and is explained below in detail with results. In this section, RL type load has been taken for comparing the performance of inverter. The experimental setup results are also taken and analyzed to validate the simulation results.

A. Inductive load with $R_{ph} = 60\Omega$ and $L_{ph} = 36 \text{ mH}$

The simulation results of inverter voltage and current waveform (with a scaling factor of 5:1) for A-phase are shown in Fig.7a. GA based program is used to find the harmonic minimized switching times for all the switches. FFT analysis for inverter voltage and current is shown in Fig.7b to the GA based harmonic minimization. From this FFT analysis, it is understood that the required fundamental voltage magnitude is controlled with reduction in the magnitude of lower order harmonics (5th, 7th and 11th). Voltage and current THD are reduced effectively and PQ is improved. The dq components of current are sharpened for the control of real power and reactive power supplied by the inverter.

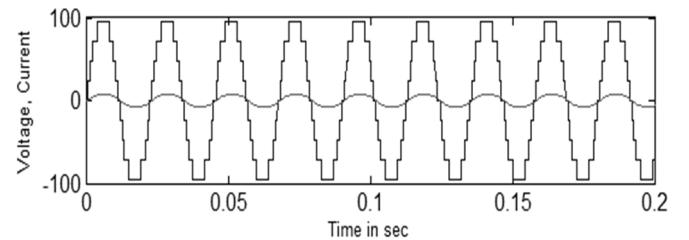


Fig 7a. Simulated waveform of Inverter voltage and current (per phase) (5:1) of A-phase with MI = 0.839

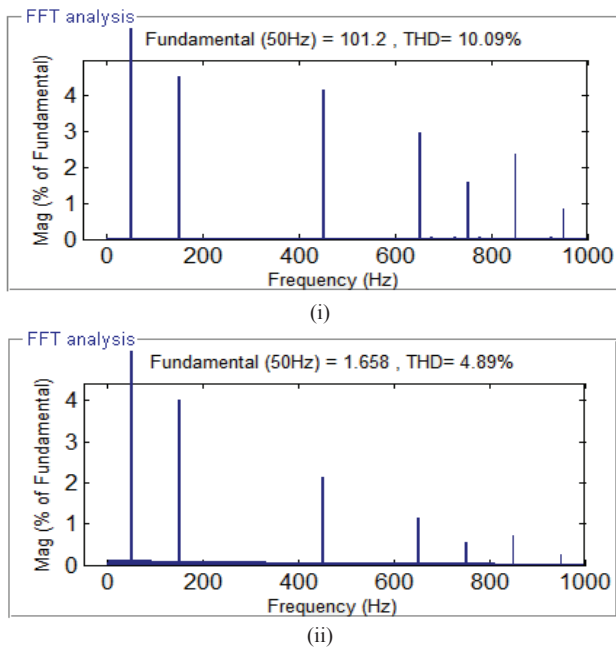


Fig 7b. Simulation results (FFT analysis) of a) voltage b) current with MI=0.839 for three-phase 17 level

Experimental results have been presented to validate the simulation results at same MI value. Fig.8 shows the snapshot of prototype experimental setup. Fig.9 shows the experimental results (Waveform patterns and FFT analysis). Harmonic values of simulation and experimental results are presented in Table V. From these values, it can be noticed that the experimental result is almost close to the simulation results obtained. The GA is functioning successfully in reducing harmonics. Fig.10a and 10b show the simulation results for three phase fifty three level inverter. Fig.11 ((i) & (ii)) shows the graphical comparison of simulated and experimental results of voltage and current at MI=0.839.

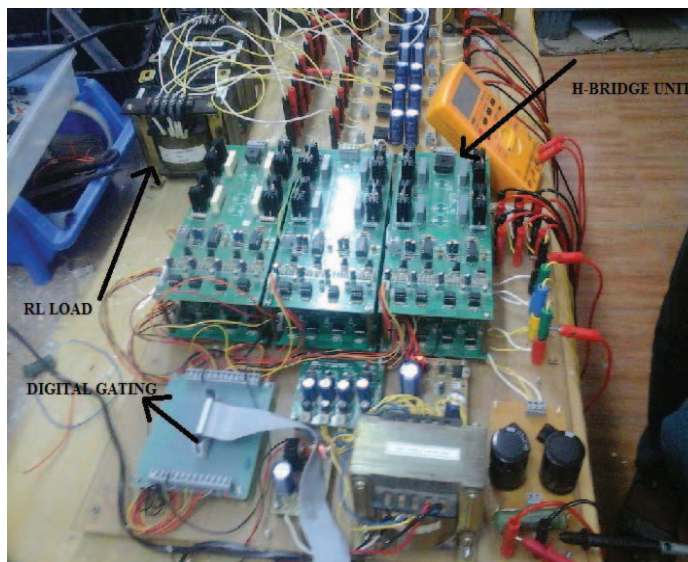


Fig 8. Prototype experimental setup of proposed ACMLI

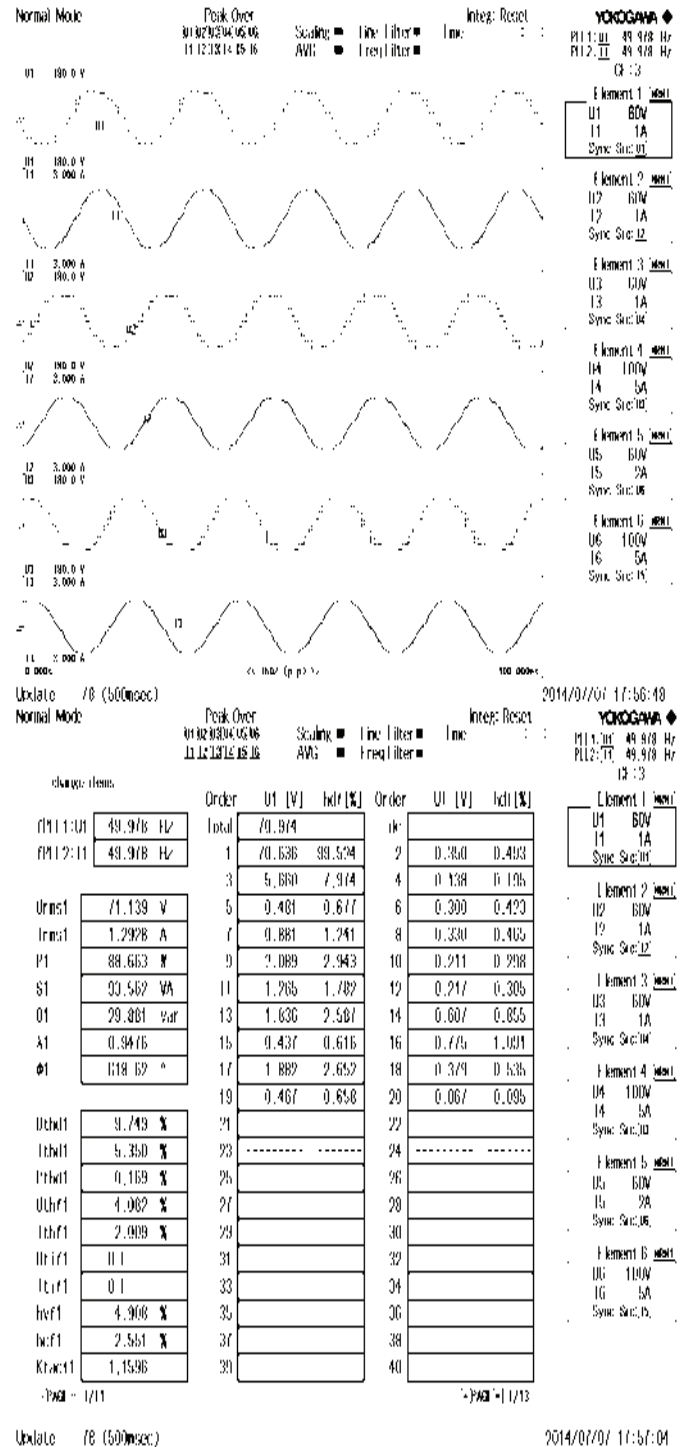


Fig 9. Experimental waveform of phase voltages, phase currents and their THD values for three-phase seventeen level

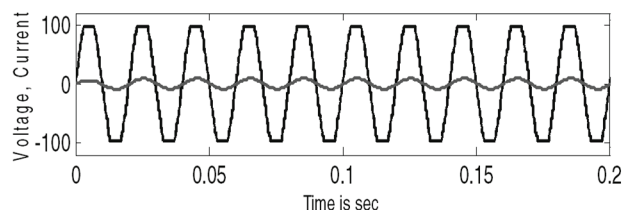


Fig 10a. Simulation results at MI=0.839 of inverter phase voltage and phase current for three-phase fifty three level

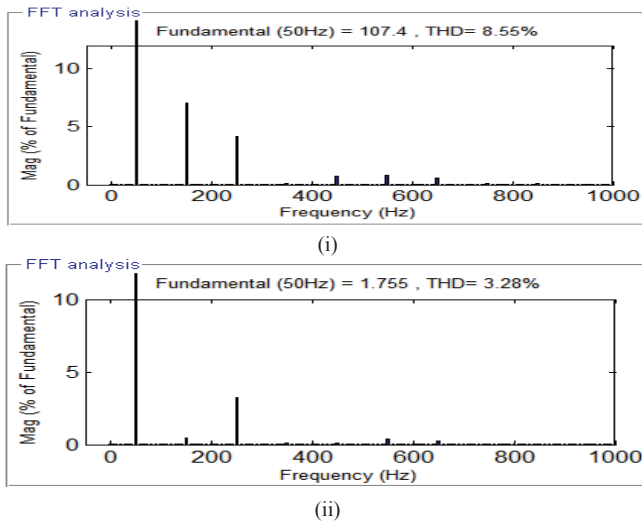
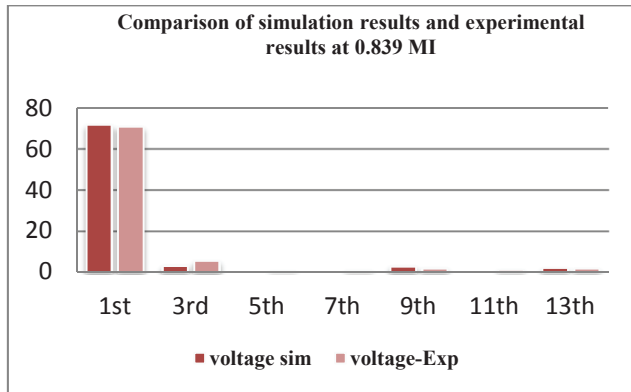


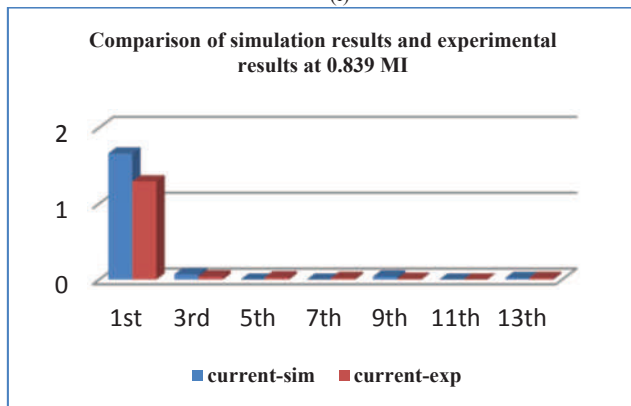
Fig 10b. Simulation results (FFT analysis) at MI=0.839 of inverter phase voltage and current for three-phase fifty three level

 TABLE V
 COMPARISON OF SIMULATION RESULTS AND EXPERIMENTAL RESULTS AT 0.839 MI FOR THREE-PHASE 17 LEVEL INVERTER

Test	Simulation		Experimental	
	voltage	current	voltage	current
Inverter Parameters	71.60	1.66	70.64	1.29
Fundamental				
3 rd	3.25	0.07	5.66	0.04
5 th	0.00	0.00	0.48	0.03
7 th	0.00	0.00	0.88	0.02
9 th	2.96	0.04	2.09	0.01
11 th	0.00	0.00	1.26	0.00
13 th	2.13	0.02	1.84	0.02
%THD	10.03	4.89	9.75	5.35



(i)



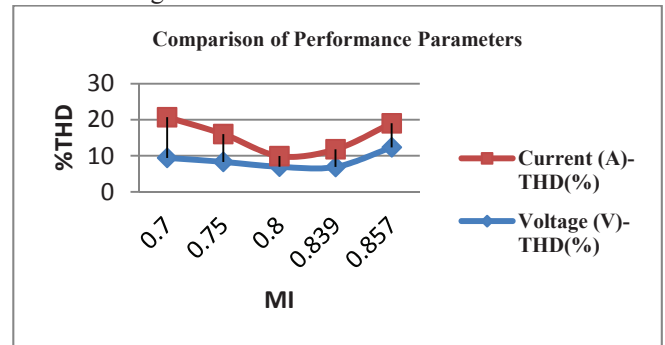
(ii)

Fig 11. Graphical representation of simulated and experimental results for (i) Voltage (ii) Current

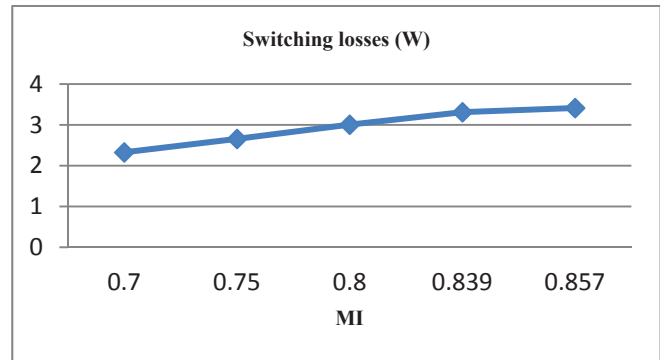
B. Inductive load with $R_{ph} = 60\Omega$ and $L_{ph} = 60\text{ mH}$

Comparisons of simulation and experimental results for three-phase 17 level inverter for MI= 0.829 are shown in Table VI.

The performance of Multilevel Inverters are compared in Table VII in terms of switching losses, efficiency, THD in output voltage and current at various MI for per phase load values of $R_{ph} = 60\ \Omega$ & $L_{ph} = 36\ \text{mH}$. The values have been taken for three phase system. The same has been presented in Fig.12 for various values of MI and the changes in switching losses and voltage current THD.



(i)



(ii)

Fig 12. Comparison of inverter performance parameters for (i) %THD (ii) Switching losses

 TABLE VI
 COMPARISON OF SIMULATION RESULTS AND EXPERIMENTAL RESULTS AT 0.829 MI FOR THREE-PHASE 17 LEVEL INVERTER

Test	Simulation		Experimental	
	voltage	current	voltage	current
Inverter Parameters	70.8	1.12	71.03	1.211
Fundamental				
3 rd	2.26	0.03	3.23	0.02
5 th	0.00	0.00	0.15	0.03
7 th	0.01	0.00	0.97	0.27
9 th	2.85	0.02	1.94	0.00
11 th	0.00	0.00	0.86	0.01
13 th	0.66	0.00	0.42	0.00
%THD	9.79	3.11	7.94	4.48

 TABLE VII
 COMPARISON OF PERFORMANCE OF INVERTER AT VARIOUS MI VALUES

MI	%THD		Switching Losses (W)
	Voltage(V)	Current(A)	
0.700	9.410	11.30	2.328
0.750	8.304	7.713	2.654
0.800	6.959	2.957	3.005
0.839	6.908	4.890	3.310
0.857	12.34	6.670	3.414

VI. CONCLUSION

Three-phase ACMLI is simulated for seventeen levels and fifty-three levels and the results are presented for two different lagging loads. The experimental results of three-phase seventeen levels ACMLI resemble the simulation results of the RL load setup. GA based algorithm has been used for switching angles calculation. It has effectively reduced the lower order harmonics and improved the Power Quality (PQ) in output (Voltage and Current) waveforms. Compared to SCMLI, the ACMLI has less number of switches for obtaining the same number of stepped AC voltage with unequal DC voltage input. In addition, the switching losses are reduced abruptly. This type of ACMLI is best suited for utility applications, electrical drives and power factor correction in grid based applications.

ACKNOWLEDGEMENT

We thank Kalasalingam University (Kalasalingam Academy of Research and Education), Krishnankoil-626 126, Ramco Institute of Technology, Rajapalayam-626 117 and MepcoSchlenk Engineering College, Sivakasi-626005 Tamil Nadu, India for having provided the experimental ambience to carry out this research work.

REFERENCES

- [1] Akira Nabae, Isao Takahashi & Hirofumi Akagi, "A new neutral point clamped PWM inverter," *IEEE Transactions on Industry Applications*, vol. IA-17, no. 5, pp. 518-523, Sep/Oct 1981.
- [2] J.S. Lai, & F.Z. Peng, "Multilevel converters-A new breed of power converters," *IEEE Transactions on Industry Applications*, vol. 32, no. 3, pp. 509-517, May/June 1996.
- [3] F.Z. Peng, "A generalized multilevel inverter topology with self-voltage balancing," *IEEE Transactions on Industry Applications*, vol. 37, no. 2, pp. 611-618, Mar/Apr 2001.
- [4] J. Rodriguez, J.S. Lai, & F.Z. Peng, "Multilevel inverters: A survey of topologies, controls, and applications," *IEEE Transactions on Industrial Electronics*, vol. 49, no. 4, pp. 724-738, Aug 2002.
- [5] K.A. Corzine, M.W. Wielebski, F.Z. Peng, & J. Wang, "Control of cascaded multi-level inverters," *IEEE Transactions on Power Electronics*, vol. 19, no. 3, pp. 732-738, May 2004.
- [6] M. Manjrekar, & T.A. Lipo, "A hybrid multilevel inverter topology for drive application," *Proceeding of the APEC 98*, 1998, pp. 523-529.
- [7] Y.S. Lai, & F.S. Shyu, "Topology for hybrid multilevel inverter," *IEE Proc. Electric Power Applications*, vol. 149, 2002, pp. 449-458.
- [8] M.D. Manjrekar, P.K. Steimer, & T.A. Lipo, "Hybrid multilevel power conversion system: a competitive solution for high-power applications," *IEEE Transactions on Industry Applications*, vol. 36, no. 3, pp. 834-841, May/June 2000.
- [9] C. Rech, & J.R. Pinheiro, "Hybrid Multilevel Converters: Unified Analysis and Design Considerations," *IEEE Transactions on Industrial Electronics*, vol. 54, no. 2, pp. 1092-1104, Apr 2007.
- [10] E. Babaei, S.H. Hosseini, G.B. Gharehpetian, M. TarafdarHaque, & M. Sabahi, "Reduction of dc voltage sources and switches in asymmetrical multilevel converters using a novel topology," *Electric Power Systems Research*, vol. 77, pp. 1073-1085, 2007.
- [11] E. Babaei, & S.H. Hosseini, "New cascaded multilevel inverter topology with minimum number of switches," *Energy Conversion and Management*, vol. 50, pp. 2761-2767, 2009.
- [12] M.R. Banaei, & E. Salary, "New multilevel inverter with reduction of switches and gate driver," *Energy Conversion and Management*, vol. 52, pp. 1129-1136, 2011.
- [13] E. Babaei, Sara Laali & Zahra Bayat, "A Single phase cascaded multilevel inverter based on a new basic unit with reduced number of switches," *IEEE Transactions on Industry Electronics*, vol. 62, no. 2, pp. 922-929, Feb 2015.
- [14] E. Babaei, "Optimal Topologies for Cascaded Sub-Multilevel Converters," *Journal of Power Electronics*, vol. 10, no. 3, pp. 251-261, May 2010.
- [15] M.R. Banaei, & E. Salary, "Asymmetric Cascaded Multi-level Inverter: A solution to obtain high number of voltage levels," *Journal of Electrical Engineering Technology*, vol. 8, no. 2, pp. 316-325, 2013.
- [16] J.N. Chiasson, L.M. Tolbert, K. McKenzie, & Z. Du, "Real-time computer control of a multilevel converter using the mathematical theory of resultants," *Elsevier J. Math. Comput. Simulation*, vol. 63, pp. 197-208, 2003.
- [17] Zhiguo Pan, & F.Z. Peng, "Harmonics optimization of the voltage balancing control for multilevel converter/ inverter systems," *IEEE Transactions on Power Electronics*, vol. 21, no. 1, pp. 211- 218, Jan 2006.
- [18] Z. Du, L.M. Tolbert, J.N. Chiasson, "Active harmonic elimination for multilevel converters," *IEEE Transactions on Power Electronics*, vol. 21, no. 2, pp. 459- 469, Mar 2006.
- [19] Burak Ozpineci, L.M. Tolbert, & John N. Chiasson, "Harmonic Optimization of Multilevel Converters Using Genetic Algorithms," *IEEE Power Electronics Letters*, vol. 3, pp. 92-95, 2005.
- [20] K. El-Naggar, & T.H. Abdelhamid, "Selective harmonic elimination of new family of multilevel inverters using genetic algorithms," *Energy Conversion and Management*, vol. 49, pp. 89-95, 2008.

Fuzzy based optimization to reduce the blind spots in heavy transport vehicles

Pitchipoo P^{a*}, Vincent D.S^b, Rajini N^c and Rajakarunakaran S^d

^a Department of Mechanical Engineering, P.S.R. Engineering College, Sivakasi, Tamil Nadu, India. Email: drpitchipoo@gmail.com

^b Tamil Nadu State Transport Corporation Ltd., Thiruvannamalai, Tamil Nadu, India.

^c Department of Mechanical Engineering, Kalasalingam University, Anand Nagar, Krishnankoil, Tamil Nadu, India.

^d Department of Mechanical Engineering, Ramco Institute of Technology, Rajapalayam, Tamil Nadu, India

Abstract:

Blind spot is a key phenomenon related to the visibility of the driver while he is driving. It plays a vital role in road accidents. Reduction of the area of blind spot is very much required in order to reduce the accidents. In this paper an attempt is made to overcome the problems of blind spot by optimizing the design parameters used in the rear view mirror design of heavy transport vehicles. The blind spot of the existing body structure was studied in a public transport corporation of Tamilnadu, India. First the area of the blind spot of the existing body structure was studied and the optimal design parameters are ranked by Fuzzy Analytical Hierarchy Process (FAHP). FAHP was also used for the determination of the weights of the design parameters and ranking of the vehicle body structures.

Keywords: Blind spots, Rear view mirror, Optimization, FAHP

1. INTRODUCTION

Statistics revealed that most of the road accidents were happened due to vision related problems of the driver. Good driver visibility results safe road traffic (Hatamleh et al., 2013). A blind spot in a vehicle is the area around the vehicle that cannot be directly seen by the driver when he is in the seat. The heavy vehicle drivers can't see some areas on the roadway in the front, behind and on either sides of the vehicle. Front side blind spots are influenced by many design criteria such as vehicle body structure, human anthropometric data, road geometry, driver seat design etc., Among the main factors to be considered for driver seat design was identified as important factor. While designing the driver's seat, height of the seat from platform, total seat height, distance of seat back rest to windscreen glass and distance of seat back rest to steering wheel centre, to reduce blind spots, the distance between seat back rest to windscreen glass attracts major importance. A large enough blind spot in the rear or sides of the heavy vehicle can completely hide a portion of pedestrian / motor-cycle or even a full vehicle. Because, blind spots hide the road to verify them before making such maneuvers on roads while turning, reversing, changing lanes, or while overtaking other vehicles. This places the driver in a risky situation resulting sometimes in untoward incidents and accidents.

Blind spots exist in a wide range of vehicles such as cars, trucks, motorboats and aircraft. Figure 1 reveals the area of the blind spot existing in a heavy transport vehicle.



Figure 1. Area of the blind spot

In this paper the blind spot on either sides of the driver while driving is considered. Rear view mirrors reduce some area of the blind spots behind and on either sides of the heavy vehicle. Adjustment and installation or positioning of mirrors with larger fields-of-view will be helpful in reducing the blind spots. While considering the installation of mirrors, the distance between the driver and the pillar or frame structure to the left and right side of the front body structure, driver eye sight height while he is in the driver seat from the platform, and the centre height of the mirror from the ground level are all the important data.

Cho and Han (2010) stated that the vision of the driver is the most vital factor for an unusual driving situation. Burger (1974) analyzed the rear vision systems in twelve passenger vehicles and three trucks under actual driving conditions and predicted the critical zone in the rear side of the vehicle using expert's opinion. Ayres et al (2005) assessed the safety aspects during the usage of rear view mirrors and analyzed the research issues involved in the design of rear view mirrors. The rear view mirrors may not be related with any significant accident prevention, possibly they are not consistently used by all the drivers while driving. More over the major accidents were caused when the target vehicle appears in the driver's blind spot during lane change or crowded urban travelling and the driver has not carefully observed the approaching vehicle from the rear and side mirrors. Pardhy et al. (2000) introduced the concept of computer graphics display driven by differential global positioning system as a virtual mirror. This display was intended to be used as a rear or side view mirror in automobiles or trucks. Kojima et al. (2005) proposed a vision support system "NaviView" as visual assistance for safe driving. Llaneras et al (2005) developed driver interface criteria for a rear obstacle detection system and evaluated various interface approaches for presenting warning information to drivers.

Fuzzy based intelligent blind spot detecting system was presented by Qidwai (2009). In this system several ultrasonic sensors were used to monitor the chosen blind spots in a vehicle. Hughes et al (2009) discussed the use of electronic vision systems in vehicles. The benefits of using wide-angle lens camera systems to minimize the vehicle's blind-zones were described. The application of RFID and bluetooth technology in the blind zone area reduction was proposed by Lakshmi and Wahida Banu (2010). Kim et al. (2011) studied the surface flow around an automotive external rear view mirror and explained the visualizations over the mirror housing surface and the driver side vehicle skin. Computer based simulation method was also used to detect and warn of objects present within the blind spots in automobiles (Hatamleh et al., 2013).

Bao et al. (2010) developed a fuzzy TOPSIS decision model for road safety using performance index by incorporating experts' opinions. This approach effectively handled experts' linguistic expressions into account in the current index research. TOPSIS was used for evaluation of road safety measures focused on road users, vehicles, road infrastructure, and comprehensive measures by using a survey with a questionnaire. An intelligent decision support system (IDSS) was developed to evaluate the road safety performance in European countries (Bao et al., 2012). To develop the IDSS, an improved hierarchical fuzzy TOPSIS model was used. The experts' knowledge was incorporated in the proposed model. FAHP method was used in several multicriteria decision making problems such as supplier evaluation and selection (Pitchipoo et al , 2013), material handling equipment selection (Kulak, 2006), machine tool selection (Taha and Rostam, 2011) etc.,

From the study of literature, it is evident that the design parameters involved in the design and installation of rear view mirror should be in the optimal conditions to overcome the problems of blind spots on the either sides of the vehicle. The aim of this work is to optimize the blind spots for heavy transport vehicles by optimizing the design parameters used for the design and implementation of rear view mirrors. To achieve this, fuzzy based decision model is developed and the model is validated by a case study conducted in the transport corporation of Tamilnadu, India. The remaining part of this paper is organized as follows: Section 2 depicts the development of model, and the case study is explained in Section 3 and finally, Section 4 concludes the study and outlines some future research directions.

2. MODEL DEVELOPMENT

In this paper the weights of the criteria and the ranking of the vehicle body structures are determined by FAHP method FAHP is developed by integrating Saaty's (1990) analytical hierarchy process with fuzzy concept. Based on the opinion of the decision maker, the evaluation criteria are compared. The ranking of the criteria used for evaluation was collected. Based on that first the criteria matrix was formed based on the Saaty's nine point scale which is shown in Table 1.

The pair wise comparison matrix is called original matrix or criteria matrix which is given by matrix X_{cri} as shown below.

$$X_{cri} = [a_{ij}]; 1 \leq i, j \leq m \quad (1)$$

where, a_{ij} = Pair wise comparison of i^{th} and j^{th} criteria. m = the number of alternatives

Table 1 Equivalent triangular fuzzy number for Saaty's nine point scale

Verbal judgment or preference	Saaty's scale of relative importance	Triangular fuzzy numbers
Extremely preferred	9	9,9,9
Very strongly to extremely preferred	8	7,8,9
Very strongly preferred	7	6,7,8
Strongly to very strongly preferred	6	5,6,7
Strongly preferred	5	4,5,6
Moderately to strongly preferred	4	3,4,5
Moderately preferred	3	2,3,4
Equally to moderately preferred	2	1,2,3

Equally preferred	1	1,1,1
-------------------	---	-------

This was converted into fuzzy original matrix using TFN prescribed by Mohamad et al. (2009) which is also shown in Table 1. The fuzzy number in a fuzzy set can be represented by equation (2).

$$F = \{x, \mu F(x), x \in R\} \quad (2)$$

where F is fuzzy set; x is fuzzy number; $R: -\alpha \leq x \leq \alpha$ and $\mu F(x)$ is a continuous mapping from R in the interval [0, 1]. A TFN expresses the relative strength of each pair of elements in the same hierarchy and denoted as TFN (M) = (l, m, u) where $l \leq m \leq u$ in which l is the smallest possible value, m is the most promising value and u is the largest possible value in a fuzzy event. The triangular membership function of M fuzzy number can be described in equation (3). Then the fuzzy original matrix is normalized using equation (4).

$$\mu_A(x) = f(x) = \begin{cases} 0 & x < l \\ (x - l)/(m - l) & l \leq x \leq m \\ (u - x)/(u - m) & m \leq x \leq u \\ 0 & x > u \end{cases} \quad (3)$$

$$N_{ij} = \frac{a_{ij}}{T_j} \quad (4)$$

where a_{ij} is the cell value of i^{th} row and j^{th} column in the fuzzy original matrix; $1 \leq i, j \leq m$; and $T_j = \sum_{i=1}^m a_{ij}$

The weights were calculated by converting fuzzy numbers into crisp values by using defuzzification technique. The defuzzification has the capability to reduce a fuzzy to a crisp single-valued quantity. There are seven methods were used for defuzzification of the fuzzy output functions such as max-membership principle, centroid method, weighted average method, mean-max membership, centre of sums, centre of largest area and first of maxima or last of maxima. In this study, centroid method was used for defuzzification which is given in equation (5).

$$\text{Weights (Crisp value)} \quad W_i = \frac{\sum_{i=1}^k D_p^i * O^i}{\sum_{i=1}^k D_p^i} \quad (5)$$

where k is the number of rules, O^i is the class generated by rule i (from 0, 1, ..., L-1); L is the number of classes and

$$D_p^i = \prod_{i=1}^n m_{li} \quad (6)$$

where n is the number of inputs and m_{li} is the membership grade of feature l in the fuzzy regions that occupies the i^{th} rule.

Since the pairwise comparison matrix is formulated based on human judgment, it is must to ensure that the values collected are accepted values. To check the consistency, the Consistency Ratio (CR) is calculated using equation (7)

$$CR = CI/RI \quad (7)$$

where CI is consistency index which is determined using equation (8) and RI is random indices for criteria size 'm'.

$$CI = \frac{\varphi_{max} - m}{m - 1} \quad (8)$$

where φ_{max} is the maximum eigen value and m is the number of criteria

RI was approximated by Saaty (1990) which is shown in Table 2. If the CR is < 0.10 the decision maker's pairwise comparison matrix is acceptable.

Table 2. Random Indices

m	1	2	3	4	5	6	7	8	9	10	11	12
RI	0	0	0.58	0.90	1.12	1.24	1.32	1.41	1.45	1.49	1.51	1.58

Then all the alternatives are compared together using Saaty's nine point scale (Table 1) based on each criterion and the pairwise matrix for alternatives are developed. This matrix is converted into fuzzy matrix using the fuzzy numbers given in Table 1. Then the fuzzy matrix is normalized using equation (4) to formulate fuzzy normalized alternative matrix. From this the weights of the alternatives based on each criterion are computed. Finally overall priority matrix is determined using equation (9).

$$O = [C_{mn}] * [W_i] \quad (9)$$

where C_{mn} is the weights of the alternative 'm' for criterion 'n'.

From the overall priority, the higher value is selected as the best alternatives

3. CASE STUDY

To prove the effectiveness of the proposed model, a case study is conducted in a transport division located in the southern part of India. At present, four different types of vehicle bodies are used in that division. They are, body built in the same organization (in-sourcing - IS) and three outsourced (OS -1, OS - 2 & OS - 3) bodies. The following data variables such as the distance between the driver and the right side of the body pillar

or frame structure (A), the distance between the driver and the left side of the body pillar or frame structure (B), the distance of driver's eye right height from the platform (C) and the distance between the centre of the rear view mirror and the ground level (D) are identified as the influencing criteria for the design and implementation of rear view mirror in heavy vehicle. The data of influencing criteria for the design of driver seat are given in Table 3.

Table 3 Data of influencing criteria for the design of driver seat

Types of Vehicle	A (cm)	B (cm)	C (cm)	D (cm)
IS	36	178	122	242
OS - 1	34	181	123	240
OS - 2	34	182	123	224
OS - 3	34	177	119	204

After the data were collected, the comparisons of criteria were obtained from the transport corporation and the same is given in Table 4.

Table 4. Crisp original matrix

	A	B	C	D
A	1	2	5	3
B	1/2	1	4	2
C	1/5	1/4	1	1/4
D	1/3	1/2	4	1

The crisp matrix is converted into fuzzy matrix using triangular fuzzy numbers (Table 1) recommended by Alias et al (2009). The fuzzy criteria matrix is shown in Table 5. The fuzzy criteria matrix was normalized and shown in Table 6. The consistency ratio for this proposed FAHP model is calculated using equation (7) and is found as 0.091 which is less than 0.1. So this model is acceptable.

Table 5. Fuzzy criteria matrix

	A			B			C			D		
A	1.000	1.000	1.000	1.000	2.000	3.000	4.000	5.000	6.000	2.000	3.000	4.000
B	1.000	0.500	0.333	1.000	1.000	1.000	3.000	4.000	5.000	1.000	2.000	3.000
C	0.250	0.200	0.167	0.333	0.250	0.200	1.000	1.000	1.000	0.333	0.250	0.200
D	0.500	0.333	0.250	1.000	0.500	0.333	3.003	4.000	5.000	1.000	1.000	1.000

Table 6. The fuzzy normalized matrix

	A			B			C			D			Weights
A	0.364	0.492	0.571	0.300	0.533	0.662	0.364	0.357	0.353	0.462	0.480	0.488	0.459
B	0.364	0.246	0.190	0.300	0.267	0.221	0.273	0.286	0.294	0.231	0.320	0.366	0.281
C	0.091	0.098	0.095	0.100	0.067	0.044	0.091	0.071	0.059	0.077	0.040	0.024	0.075
D	0.182	0.164	0.143	0.300	0.133	0.074	0.273	0.286	0.294	0.231	0.160	0.122	0.210

Table 7. Fuzzy alternative matrix

		IS			OS - 1			OS - 2			OS - 3		
Based on A	IS	1.000	1.000	1.000	0.250	0.200	0.167	0.250	0.200	0.167	0.250	0.200	0.167
	OS - 1	4.000	5.000	5.988	1.000	1.000	1.000	1.000	1.000	1.000	1.000	1.000	1.000
	OS - 2	4.000	5.000	5.988	1.000	1.000	1.000	1.000	1.000	1.000	1.000	1.000	1.000
	OS - 3	4.000	5.000	5.988	1.000	1.000	1.000	1.000	1.000	1.000	1.000	1.000	1.000
Based on B	IS	1.000	1.000	1.000	0.500	0.333	0.250	0.250	0.200	0.167	2.000	3.000	4.000
	OS - 1	2.000	3.003	4.000	1.000	1.000	1.000	2.000	3.000	4.000	4.000	5.000	6.000
	OS - 2	4.000	5.000	5.988	0.500	0.333	0.250	1.000	1.000	1.000	6.000	7.000	8.000
	OS - 3	0.500	0.333	0.250	0.250	0.200	0.167	0.167	0.143	0.125	1.000	1.000	1.000
Based on C	IS	1.000	1.000	1.000	2.000	3.000	4.000	2.000	3.000	4.000	0.500	0.333	0.250
	OS - 1	0.500	0.333	0.250	1.000	1.000	1.000	1.000	1.000	1.000	0.250	0.200	0.167
	OS - 2	0.500	0.333	0.250	1.000	1.000	1.000	1.000	1.000	1.000	0.250	0.200	0.167
	OS - 3	2.000	3.003	4.000	4.000	5.000	5.988	4.000	5.000	5.988	1.000	1.000	1.000
Based on D	IS	1.000	1.000	1.000	0.500	0.333	0.250	0.200	0.167	0.143	0.111	0.111	0.111

OS - 1	2.000	3.003	4.000	1.000	1.000	1.000	0.250	0.200	0.167	0.111	0.111	0.111
OS - 2	5.000	5.988	6.993	4.000	5.000	5.988	1.000	1.000	1.000	0.167	0.143	0.125
OS - 3	9.009	9.009	9.009	9.009	9.009	9.009	6.000	7.000	8.000	1.000	1.000	1.000

After checking the consistency, the weights of the criteria are determined using equation (5) and shown in Table 6. Next the alternatives are compared with each other based on all selected criteria which are shown in Table 7. Then these fuzzy matrixes are normalized and shown in Table 8. Finally the overall priority is determined using equation (9). From the overall priority the best alternative is selected. Table 9 depicts the overall priority for all the alternatives.

Table 8. Normalized alternative matrix

		IS			OS - 1			OS - 2			OS - 3			Score
Based on A	IS	0.077	0.063	0.053	0.077	0.063	0.053	0.077	0.063	0.053	0.077	0.063	0.053	0.064
	OS - 1	0.308	0.313	0.316	0.308	0.313	0.316	0.308	0.313	0.316	0.308	0.313	0.316	0.312
	OS - 2	0.308	0.313	0.316	0.308	0.313	0.316	0.308	0.313	0.316	0.308	0.313	0.316	0.312
	OS - 3	0.308	0.313	0.316	0.308	0.313	0.316	0.308	0.313	0.316	0.308	0.313	0.316	0.312
Based on B	IS	0.133	0.107	0.089	0.222	0.178	0.150	0.073	0.046	0.032	0.154	0.188	0.211	0.156
	OS - 1	0.267	0.322	0.356	0.444	0.536	0.600	0.585	0.691	0.756	0.308	0.313	0.316	0.509
	OS - 2	0.533	0.536	0.533	0.222	0.179	0.150	0.293	0.230	0.189	0.462	0.438	0.421	0.408
	OS - 3	0.067	0.036	0.022	0.111	0.107	0.100	0.049	0.033	0.024	0.077	0.063	0.053	0.074
Based on C	IS	0.250	0.214	0.182	0.250	0.300	0.334	0.250	0.300	0.334	0.250	0.192	0.158	0.259
	OS - 1	0.125	0.071	0.045	0.125	0.100	0.083	0.125	0.100	0.083	0.125	0.115	0.105	0.102
	OS - 2	0.125	0.071	0.045	0.125	0.100	0.083	0.125	0.100	0.083	0.125	0.115	0.105	0.102
	OS - 3	0.500	0.643	0.727	0.500	0.500	0.500	0.500	0.500	0.500	0.500	0.577	0.631	0.553
Based on D	IS	0.059	0.053	0.048	0.034	0.022	0.015	0.027	0.020	0.015	0.080	0.081	0.082	0.058
	OS - 1	0.118	0.158	0.190	0.069	0.065	0.062	0.034	0.024	0.018	0.080	0.081	0.082	0.109
	OS - 2	0.294	0.315	0.333	0.276	0.326	0.369	0.134	0.120	0.107	0.120	0.105	0.093	0.265
	OS - 3	0.530	0.474	0.429	0.621	0.587	0.555	0.805	0.837	0.859	0.720	0.733	0.742	0.686

Table 9 Overall priority score

	A	B	C	D	Overall Score
IS	0.029	0.044	0.020	0.012	0.105
OS - 1	0.143	0.143	0.008	0.023	0.317
OS - 2	0.143	0.114	0.008	0.056	0.321
OS - 3	0.143	0.021	0.042	0.144	0.350

From Table 9 & Figure 2, OS - 3 vehicle has the higher score (FAHP score) values followed by OS - 2, OS - 1 & IS body built vehicles.

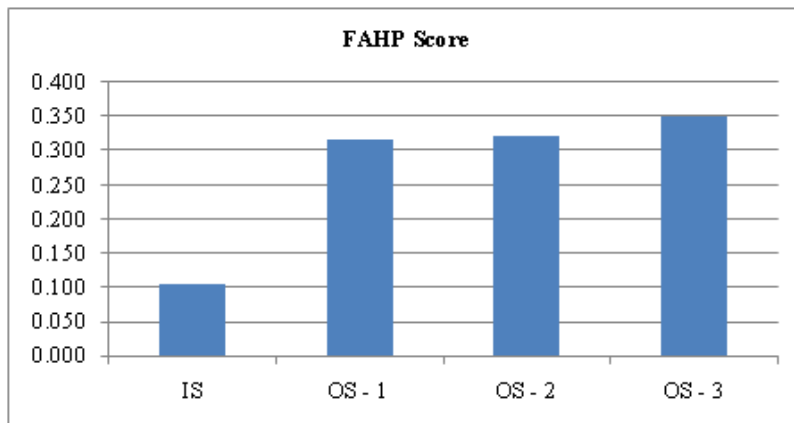


Figure 2. FAHP score

4. CONCLUSION

This paper discusses the elimination of blind spots in the sides and rear side of the heavy vehicle which is an important aspect of road safety. An intelligent multi criteria optimization model was proposed in the reduction of blind spot area in heavy transport vehicle. FAHP was used to determine the weights of the influencing criteria and the best alternative was also selected. In the model fuzzy concepts are combined with AHP. The model was tested by a case study and the effectiveness of the model was proved. FAHP is an effective tool which can accommodate both tangible and intangible factors. Based on the suggestion of optimized positioning of rear view mirror, there are great chances of reduction of area of blind spots in the sides and rear of the heavy vehicle.

REFERENCES

1. Hazem (Moh'd Said) Hatamleh, Ahmed A.M Sharadqeh, As'ad Mahmoud Alnaser, Omar Alheyasat and Ashraf Abdel-Karim Abu-Ein (2013). Computer simulation to detect the blind spots in automobiles. *International Journal of Computer Science Issues*, 10 (1), 453-456.
2. Burger W. (1974). Evaluation of innovative passenger car and truck rear vision system. SAE paper 1974 – 740965.
3. Thomas Ayres, Li Li, Doris Trachtman and Douglas Youn. (2005). Passenger-side rear-view mirrors: driver behavior and safety. *International Journal of Industrial Ergonomics*, 35, 157–162.
4. Pardhy S., Shankwitz C. and Donath M. (2000). A virtual mirror for assisting drivers. *The Proceedings of IEEE symposium on Intelligent Vehicles*, Dearborn, Michigan, USA: 255 – 260.
5. Kojima K., Sato A., Taya F., Kameda Y. and Ohta Y. (2005). Naviview: visual assistance by virtual mirrors at blind intersection. *The Proceedings of IEEE Intelligent Transportation Systems*, Vienna, Austria: 592 – 597.
6. Qidwai U. (2009). Fuzzy blind-spot scanner for automobiles. *The Proceedings of IEEE Symposium on Industrial Electronics & Applications*, Kuala Lumpur, Malaysia: 758 – 763.
7. Hughes C., Glavin M., Jones E. and Denny P. (2009). Wide-angle camera technology for automotive applications: A review. *Intelligent Transport System*, 3(1), 19-31.
8. Lakshmi S. and Wahida Banu R.S.D. (2010). Efficient realisation and rendering of images in blind zone. *Journal of Computer Engineering*, 1(1), 1-5.
9. Cho Y.H. and Han B.K. (2010). Application of slim a-pillar to improve driver's field of vision. *International Journal of Automotive Technology*, 1 (4), 517-524.
10. Kim J.H., Park B.H. and Han Y.O. (2011). Surface flow and wake characteristics of automotive external rear-view mirror. *Proceedings of the Institution of Mechanical Engineers Part D - Journal of Automobile Engineering*, 225 (12): 1605-1613.
11. Qiong Bao, Da Ruan, Yongjun Shen, and Elke Hermans. (2010). Creating a composite road safety performance index by a hierarchical fuzzy TOPSIS approach. *The Proceedings of International Conference on Intelligent Systems and Knowledge Engineering*, Hangzhou, China: 458-463.
12. Qiong Bao, Da Ruan, Yongjun Shen, Elke Hermans and Davy Janssens. (2012). Improved hierarchical fuzzy TOPSIS for road safety performance evaluation. *Knowledge Based Systems*, 32, 84-90.
13. Robert E. Llaneras, Charles A. Green, Raymond J. Kiefer, William J. Chundrlik Jr., Osman D. Altan and Jeremiah P. Singer. (2005). Design and evaluation of a prototype rear obstacle detection and driver warning system. *Human Factors*, 47 (1), 199-215.
14. Pitchipoo P., Venkumar P. and Rajakarunakaran S. (2013). Fuzzy hybrid decision model for supplier evaluation and selection. *International Journal of Production Research*, 51 (13), 3903-3919.
15. Osman Kulak. (2005). A decision support system for fuzzy multi-attribute selection of material handling equipments. *Expert Systems with Applications*, 29, 310–319.
16. Zahari Taha and Sarkawt Rostam. (2011). A fuzzy AHP–ANN-based decision support system for machine tool selection in a flexible manufacturing cell. *International Journal of Advanced Manufacturing Technology*, 57 (5-8), 719–733.
17. Thomas L. Saaty. (1990). How to make a decision: the analytic hierarchy process. *European Journal of Operations Research*, 48 (1), 9-26.
18. Mohamad Ashari Alias, Siti Zaiton Mohd Hashim and Supiah Samsudin. (2009). Using fuzzy analytic hierarchy process for southern Johor river ranking. *International Journal of Advanced Soft Computing Applications*, 1 (1), 62-76

PEC-DM-232

DAMAGE DETECTION OF COST EFFECTIVE CFRP COMPOSITE STRUCTURE USING FIBER OPTIC SENSOR UNDER DYNAMIC LOAD

J. Jerold John Britto^{1, a}, A. Vasanthanathan^{2, b}, Dr. P. Nagaraj^{3, c}

¹Assistant Professor, Department of Mechanical Engineering, Ramco Institute of Technology, Rajapalayam, India

²Associate Professor, Department of Mechanical Engineering, Mepco Schlenk Engineering College, Sivakasi, India

³Sr. Professor & Head, Department of Mechanical Engineering, Mepco Schlenk Engineering College, Sivakasi, India

Abstract: Recent advances and cost reductions has simulated interest in fiber optical sensing. This technique helps to detect the damage in aircraft structure. Nowadays, most of the critical components of aircraft structure made up of composite structure. CFRP can significantly reduce the weight while increasing strength and durability. The weight reduction of the structure will increase the fuel efficiency. The composite structure subjected to static and dynamic loading during the running condition. This paper overviews the cost effective material selection (CFRP) and damage detection setup using fiber optic sensor under dynamic loading condition. The spectrum received from the damage detection setup is analysed to ensure the size, shape and damage condition. The intensity of spectrum depends on the damage size of the given component. The entire paper shows the damage detection under dynamic loading with various indenter for impact.

Keywords: Fiber optic sensor, Composite Laminate, CFRP, Impact.

I. Introduction

Carbon-fiber-reinforced polymers are composite materials. They have unique properties of relatively high strength at high temperatures coupled with low thermal expansion and low density [1]. The physical properties of composite materials are generally not isotropic in nature, but rather are typically anisotropic (different depending on the direction of the applied force or load). For instance, the stiffness of a composite panel will often depend upon the orientation of the applied forces and/or moments.

Static and Dynamic loads are known to induce damage to the composite in the form of matrix cracking delamination, debonding and fibre breakage (Serge Abrate, 2011). Research has shown that composites are capable of absorbing energy and dissipating it by various fracture and elastic processes when subjected to a loads. The ability of composite material is to absorb energy elastically depends on the mechanical properties of the matrix and fibres, the interfacial strength, the velocity of impact (Hualin Fan et al., 2009) and the size of the component. Materials and structures, in addition to enabling technologies for future aeronautical and space systems, continue to be the key elements in determining the reliability, performance, testability, and cost effectiveness of these systems. The focus of the present paper is on developments damage identification using fiber optic sensor.

II. MATERIALS AND METHODS

1. MATERIALS

a. Carbon Fibre

Carbon fibers are commercially available with a variety of tensile modulus values ranging from 207 MPa on the low side to 1035 MPa on the high side. In general, the low-modulus fibers have lower density, lower cost, higher tensile and compressive strengths, and higher tensile strains-to-failure than the high-modulus fibers.

Carbon fibers are their exceptionally high tensile strength–weight ratios as well as tensile modulus–weight ratios, very low coefficient of linear thermal expansion high fatigue strengths, and high thermal conductivity. Their high cost has so far excluded them from widespread commercial applications. They are used mostly in the aerospace industry, where weight saving is considered more critical than cost.

b Epoxy Resin & Hardener

Epoxy resins are the most used just after polyesters, their price being the only limit to their usage. They have better mechanical characteristics in tension, compression, impact and others when compared with polyester resins, and so they are preferred in the manufacturing of high performance parts like those used in aeronautics and others. Besides they present good heat resistance up to 150° to 190° C, have good chemical resistance, [2] low retraction, good reinforcement wetting and an excellent adhesion to metallic materials. The hardener is used to cure the matrix materials in fibre as faster than usual curing time. From that we can get excellent adhesive bonding together and normally the proportion of hardener, epoxy resin is equal amount and equal to weight of fibre.

c. Fiber Optic Sensor

Fiber optic sensor technology has been a major user of technology associated with the optoelectronic and fiber optic communications industries. The ability of fiber optic sensors to displace traditional sensors (Shizhuo Yin, Paul B. Ruffin, Francis T. S. Yu 2008) for rotation, acceleration, electric and magnetic field measurement, temperature, pressure, acoustics, vibration, linear and angular position, strain, humidity, viscosity, chemical measurements, and a host of other sensor applications has been enhanced. The inherent advantages of fiber optic sensors, which include their ability to be lightweight, of very small size, passive, low power, and resistant to electromagnetic interference, high sensitivity [9].Fiber optic sensors are often loosely grouped into two basic classes referred to as extrinsic, or hybrid, fiber optic sensors and intrinsic, or all fiber, sensors.

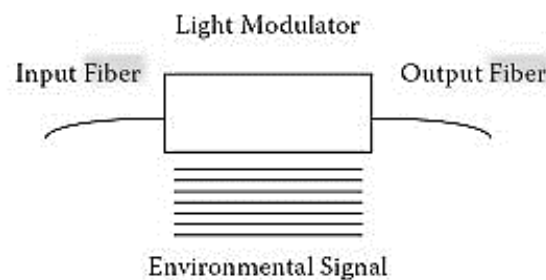


Fig. 1 Overview of Fiber Optic Sensors.

d. Material Properties

The following material properties from Test Data results [3,4] have been taken into account for analysis 1 Psi = 0.0069 MPa. Composites are the orthotropic material the property varies along the three directions. The stiffness of a composite panel will often depend upon the orientation of the applied forces and/or moments. Panel stiffness is also dependent on the design of the panel.

Table 1 Material Property of CFRP

Properties		Carbon/epoxy
E _a	(GPa)	125.485
E _b	(GPa)	8.067
E _c	(GPa)	8.067
G _{ab}	(GPa)	41.29
G _{bc}	(GPa)	2.42
G _{ca}	(GPa)	4.129
γ_{ba}		0.0176
γ_{cb}		0.0176
γ_{ca}		0.4657
Density	Kg/m ³	4.152

III. EXPERIMENTATION

3.1 Low velocity impact test Data

Damage in unidirectional carbon/fibre composite resulting from low velocity/energy impacts was evaluated embedded fiber optic sensor. [6] The value for conducting experiments based on the experimental results taken from the output of the experimental value the Impactor and energy consideration taken into account for the further improvement of the velocity impact energy. Initially low velocity impact was conducted by using two types of impactor shape [7]. The laminates used in the low velocity impact tests were manufactured from uni-directional carbon fibre/epoxy prepreg. The panels 200 mm × 90 mm × 3 mm.

1. Impactor for testing
 - Conical -167gm
 - Hemi Spherical -180 gm
2. Impact Energy for conducting test
 - 0.33 J with Corresponding velocity 1.3 m/s
 - 0.56 J with corresponding velocity 2.5 m/s
3. Formula for calculating the impact energy
 - $E=W \times h$

$V = \sqrt{2gh}$ Where W- Weight of the Impactor (N), h- Vertical height,

Courtesy: "Evaluating impact damage in CFRP using fibre optic sensors" A.R. Chambers *a,**, M.C. Mowlem *b*, L. Dokos *a*

V- velocity (m/s), E – Energy (J)

3.2 Experimental Setup

Figure 2 – 4 shows the configuration of the test specimen of impact detection with flat plat. The specimen is a quasi-isotropic laminate plate. A single mode fiber sensor was bonded to the specimen surface for impact damage detection. The following components are used for the experiments (a) Electrical Input Signal – 1MHz, (b) Optical Transmitter, (c) Single mode fiber cable, (d) Optical receiver, (e) Digital Oscilloscope with data acquisition system. The low velocity impact experimental setup was created for damage detection.

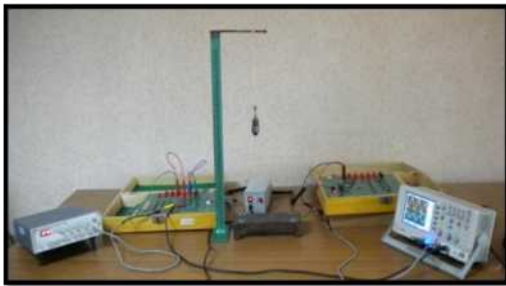


Fig. 2 Dynamic Load Test Setup Arrangement



Fig. 3 Test Setup arrangement

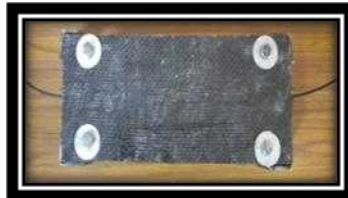


Fig. 4 Test Specimen with fiber optic sensor

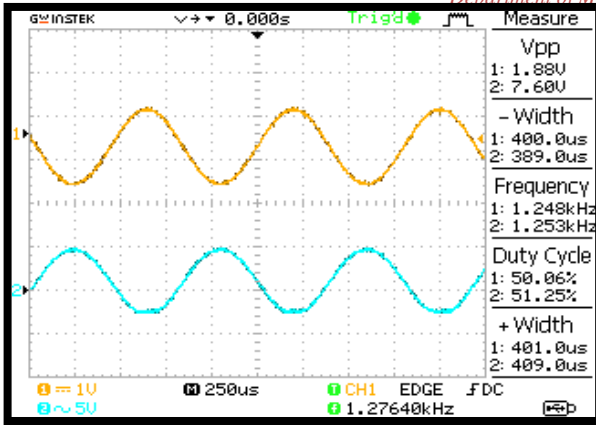


Fig (3) h= 186.88mm at 0.33J Hemi Spherical Impactor

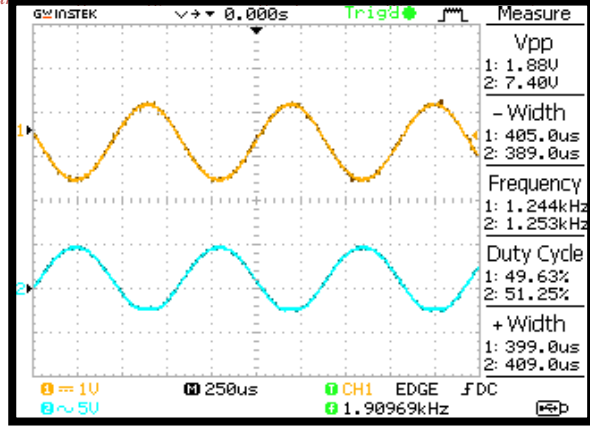
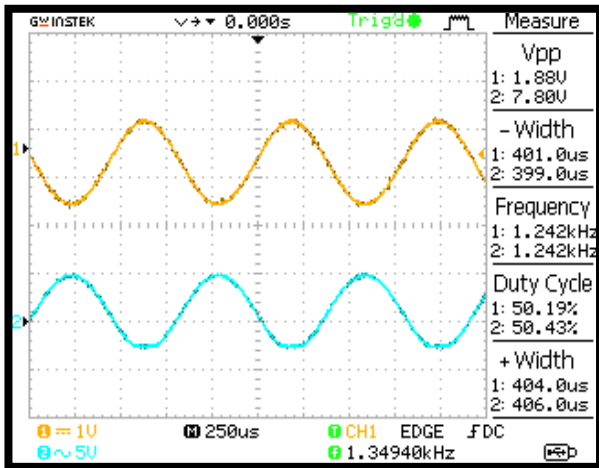


Fig (4) h= 317.1 mm at 0.56J Hemi Spherical Impactor

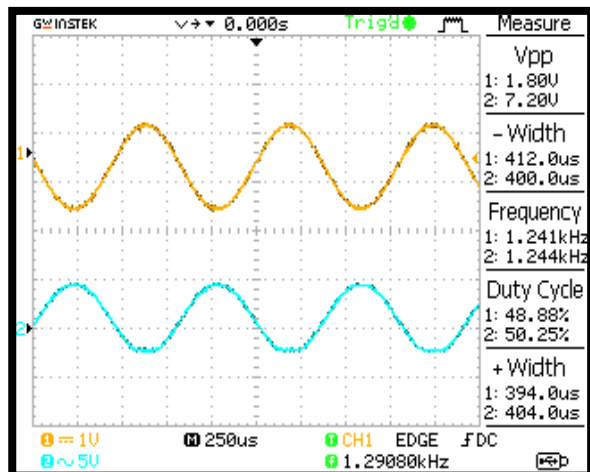
IV. RESULTS AND DISCUSSIONS

The following experimental result graph shows that the various impact energy with

Fig (2) h= 341.4mm at 0.56J Conical Impactor



respect to the various height level [8]. Fig (1) h= 201.4mm at 0.33J Conical Impactor



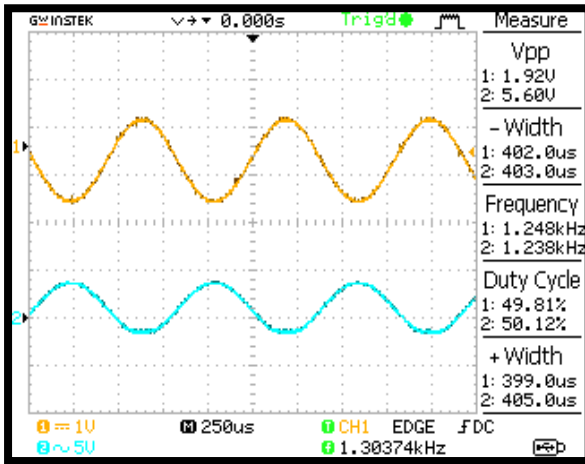


Fig (5) h= 320.4mm at 0.33J Conical Impactor (Ø 12mm)

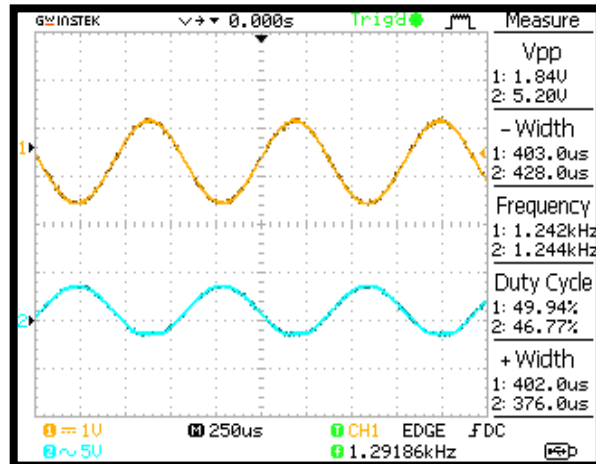


Fig (6) h= 543.66mm at 0.56J flat Impactor (Ø 12mm)

Fig. 5 Output Results for Dynamic Analysis

The damage detection principle of this system is based on the energy change of the received waveform. If a damaged section exists in the path of the elastic wave, the energy of the elastic wave will change. By detecting this change, the system can detect the damage in a composite structure. We could successfully detect the damage propagation by this system. Figure 5 [1-6] shows an output wave form of the impact load condition. We have conducted the impact detection test using a drop-weight type impact machine.

The weight of was 167 gm and its tip was a conical shape. The energy of the impact is 0.33 J at velocity 1.3 m/s. The figures 5 [1,3,5] shows the received waveform and the enlarged waveform of the elastic wave of fiber optic sensors under 0.33 J energy with height range of 201.6 mm, 186.88 mm and 320.4 mm. The figures 5 [2,4,6] shows the received waveform and the enlarged waveform of the elastic wave of fiber optic sensors under 0.56 J energy with height range of 341.4 mm, 317.1 mm and 543.6 mm. Based on this output wave the experimental setup detect the resulting damage. As the result of this study, it was revealed that two kind of detections, damage monitoring and impact detection, with the same system construction by the damage monitoring using single mode fiber sensor.

V. CONCLUDING REMARKS

The following conclusions were drawn from the present experimental investigations:

1. Carbon fibre is suitable material for absorbing more energy during the impact loading condition. Based on the material property.
2. For the constant input voltage of 1.88v the output voltage varies with respect to the impact [Fig. 5 (1 – 6)] load energy of 0.56 J, the output voltage is 5.20v.
3. The shape of the impactor in this experimental work: conical, Hemi spherical and flat shape.
4. In this paper, the low velocity impact load is applied in between the range of 1.3 to 2.5 m/s.

5. The figure 5 [1 – 5] shows the output of the impact load on the composite plate and it shows the energy absorption capability of carbon fiber material.

ACKNOWLEDGEMENT

All the praise goes to Almighty God for his source of all inspirations, for showering his divine and merciful blessings on us. We express our heartiest gratitude and the authors would like to thank The Principal/RAMCO Institute of Technology, Rajapalayam and The Principal/MEPCO SCHLENK Engineering College, Sivakasi for providing facilities to carry out this research work.

REFERENCES

- [1] Deborah D.L. Chung, "Composite Materials Functions and modern Technologies" composite materials laboratory, University of Buffalo, New York, 2009..
- [2] P. K. Mallick, "Fiber-Reinforced Composites: Materials, Manufacturing and Design" – Taylor & Francis Group, LLC.
- [3] G. C. Sih and S. E. Hsu, "Advanced Composite Materials and Structures" – Publisher VNU Science Press BV.
- [4] Kersey AD, Davis MA, Patrick HJ, LeBlanc M, Koo KP, Askins CG, Putnam MA, and Friebele EJ. Fiber grating sensors, Journal of Lightwave Technol., Vol.15, No. 8, pp 1442-1463, 1997.
- [5] Satori K, Fukuchi K, Kurosawa Y, Hongo A, and Takeda N. Polyimide-coated small-diameter optical fiber sensors for embedding in composite laminate structures, Proc. SPIE, Vol. 4328, pp 285-294, 2001.
- [6] Okabe Y., Mizutani, T, Yashiro S, and Takeda N. Detection of microscopic damages in composite laminates with embedded small-diameter fiber Bragg grating sensors. Comp. Sci. Technol., Vol. 62, No. 7-8, pp 951-958, 2002.
- [7] Guemes JA and Menendez JM. Response of Bragg grating fiber-optic sensors when embedded in composite laminates. Comp. Sci. Technol., Vol. 62, No. 7-8, pp 959-966, 2002.
- [8] Taketa I, Amano M, Okabe Y, and Takeda N. Damage detection and suppression system of CFRP laminates with FBG sensor and SMA actuator. Trans. Mater. Res. Soc. Japan, Vol. 28, No. 3, pp 675-678, 2003.
- [9] Shizhuo Yin, Paul B. Ruffin and Francis T. S. Yu, "Fiber Optic Sensors", CRC Press, Taylor & Francis Group.



International Conference on
Magnetic Materials and Applications

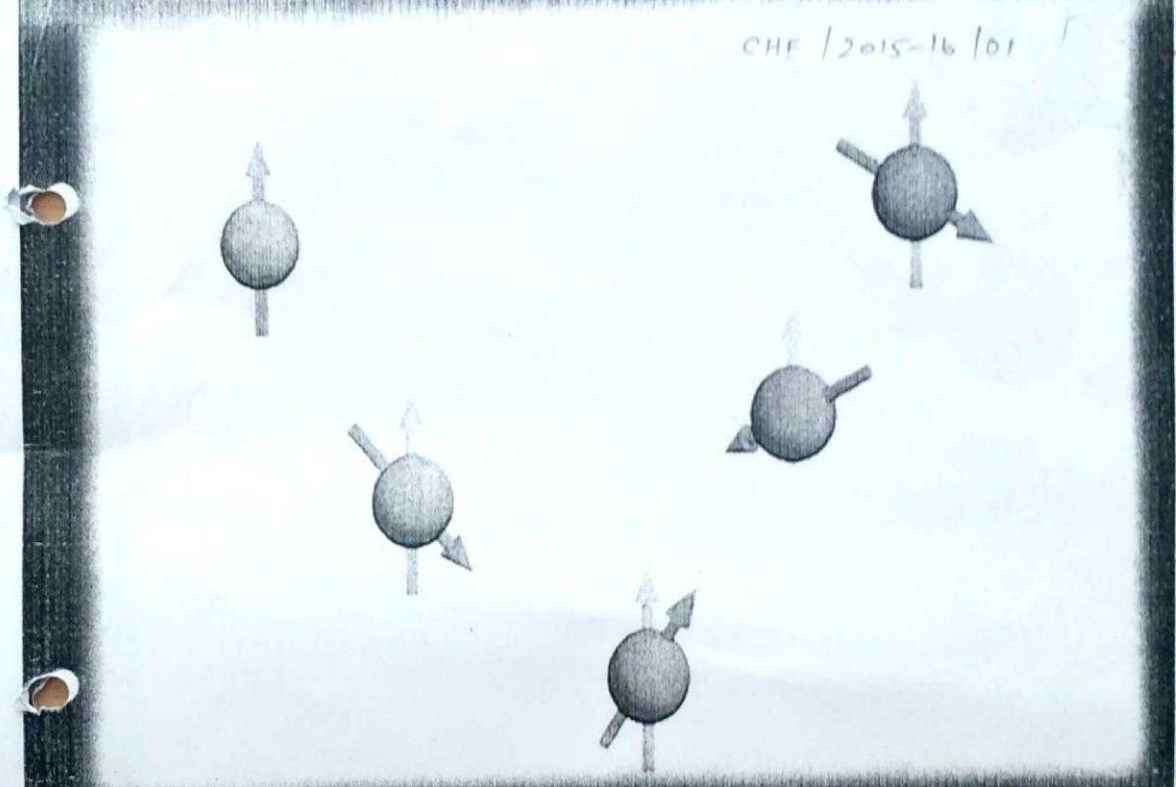


ICMAGMA - 2015

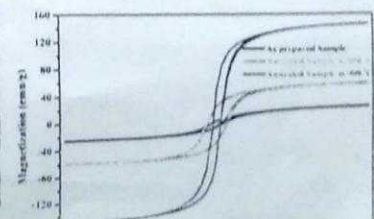
SOUVENIR & ABSTRACTS

www.vit.ac.in/icmagma2015

CHE / 2015-16 / 01



Organized by
School of Advanced Sciences
VIT University, Vellore
&
Magnetics Society of India



I28: Adsorption Studies for the Removal of Ni(II), Co(II), Cu(II) And Pb(II) Ions using Synthetic Nano Iron Oxide (SNIO)

G. Kanthimathi^{1,*}, P. Kotteeswaran² and M. Kottaisamy³

¹Department of Chemistry, Ramco Institute of Technology, Rajapalayam 626 117.

²Department of Chemistry, Renganayaki Varatharaj College of Engineering, Sivakasi, 626 128.

³Department of Chemistry, Thiagarajar College of Engineering, Madurai, India 625 015

* Email: kanthi_somu@rediffmail.com

compare the sorption behaviour of SNIO towards the Ni(II), Co(II), Cu(II) and Pb(II) ions. The study was conducted on the basis of parameters such as a function of initial concentration of the adsorbate, adsorbent dosage, contact time and pH. Freundlich and Langmuir isotherm models have been tested. The applicability of various first order kinetic equations like Natarajan-Khalaf, Lagergren, Elovich and Power functions equations were tested. The optimum conditions of the various factors for the maximum removal of the above mentioned metal ions was found out and compared.

Abstract

The adsorbent Synthetic Nano Iron Oxide (SNIO) was synthesized and essential characteristics were ascertained using XRD, FT-IR, SEM, and EDAX techniques. Adsorption experiments were carried out by using Batch method to

found to be hydrophobic in nature. This is confirmed by measurement of contact angles. This hydrophobic film can be coated on the water proof rain coat, caps, shoes etc. to create water repellent surfaces.

Key words: Self-assembled mono layers, carbon steel, Tween 20, hydrophobicity, AC-impedance spectra, AFM, contact angle, FTIR

OP-5

BIOLOGICAL EVALUATION OF TRANSITION METAL COMPLEXES USING PYRIMIDINE DERIVATIVE: SYNTHESIS, CHARACTERISATION, DNA BINDING AND CLEAVAGE ACTIVITY

N.Revathi^{a,b} and J.Dhaveethu Raja^{*c}

^aDepartment of Chemistry, Ramco Institute of Technology, Rajapalayam - 626117.

^bDepartment of Chemistry, Manonmanium Sundaranar University, Tirunelveli - 627 012. ^{*c}Chemistry Research Centre, Mohamed Sathak Engineering College, Kilakarai - 623 806.

E-mail: ^cjdrajapriya@gmail.com, ^{a,b}nrevathivijay@gmail.com

Abstract

A new series of transition metal complexes of Cu(II) and Zn(II) had been synthesised from the pyrimidine derivative Schiff base 2-((4-amino-6-chloropyrimidin-2-(amino)methyl)-4-nitrophenol). Structural features had been arrived from their elemental analyses, molar conductance, mass, IR, UV-Visible, ¹H-NMR and ESR spectral studies. The UV-Visible and ESR spectral data of the complexes suggested an octahedral geometry around the central metal ion. The antibacterial activity of the Schiff base and its complexes had been extensively studied on microorganisms such as gram positive bacteria like as *Staphylococcus aureus*, *Streptococcus pneumoniae*, *Staphylococcus pneumoniae*, *Bacillus subtilis* and gram negative bacteria like as *Shigella flexneri*, *Salmonella thypi*, *Klebsiella pneumoniae*, *Haemophilus influenzae*. The result indicated that zinc complex had mild antibacterial activity against the microorganisms. DNA cleavage activity of the Schiff base and its complexes with calf thymus DNA (CT DNA) had been carried out using Gel electrophoresis technique. The interaction of the copper(II) and zinc(II) complexes was studied by absorption spectroscopy, which revealed that the complexes could interact with herring sperm DNA (HS DNA) through an intercalation mode with binding constant $1.94 \times 10^3 - 1.45 \times 10^4 \text{ M}^{-1}$.

Keywords: Pyrimidine derivative, Antibacterial activity, DNA cleavage, DNA binding.

